Technology Collaboration Programme
by IEA

TECHNICAL REPORT

Workshop on Tidal Current Extractable Energy: Modelling, Verification and Validation

August 2023

PREPARED FOR:

International Energy Agency' Ocean Energy Systems Technology Collaboration Programme

OES OCEAN ENERGY SYSTEMS

NANYANG TECHNOLOGICAL UNIVERSITY SINGAPORE

IEA-OES Technology Collaboration Programme

IEA-OES is a Technology Collaboration Programme on Ocean Energy Systems within the International Energy Agency (IEA). Technology Collaboration Programmes are independent, international groups of experts that enable governments and industries from around the world to lead programmes and projects on a wide range of energy technologies and related issues.

AUTHORED BY:

Dr. Narasimalu Srikanth, Nanyang Technological University, Singapore
Dr. Jerome Thiebot, Université de Caen Normandie, France
Mr. Kannappan Lakshmanan, Nanyang Technological University, Singapore
Dr. Ahmad Firdaus, Bandung Institute of Technology, Indonesia
Dr. Kadir Orhan, Christian-Albrechts-Universität zu Kiel, Germany
Prof. Ye Li, Shanghai jiao tong university, China

CONTACT:

Dr. Srikanth Narasimalu,
Program Director / Principal Research Scientist
Email: NSRIKANTH@ntu.edu.sg
1 Clean Tech Loop, #06-04 Clean Tech One Bldg. Singapore 637141
Tel: +65 6592 1674, Fax: +65 6694 621

Disclaimer

Citation

IEA-OES (2023), Technical Report “Workshop on Tidal Current Extractable Energy: Modelling, Verification and Validation”. www.ocean-energy-systems.org

Contents

1. Introduction

Knowing the fact that majority of the earth is covered with water, the extraction of tidal energy to generate electricity is augmenting interests of the researchers and the method is being further enhanced. In the evaluation of tidal power resources, cataloguing of appropriate sites and estimation of achievable energy are greatly important. Nations with long coastlines, having features like bays, estuaries etc., create a variation in the tidal currents. Also, these coastline properties possess high current velocities making them suitable sites for converting tidal energy in electrical energy. Models are being developed to identify the locations with high flow velocities and later analyzing those areas for the average power density. In this way, sites are being identified for installing tidal power plants. However, the correctness of these models is a function of the accuracy and the resolution of the input data required for these models. Further, the certainty also depends on the hydrodynamic phenomenon being examined by the various models to simulate the ocean flow. Like certain models, does 3-dimensional simulation while other does a 2-dimensional depth-averaged simulation. Still, these models serve the purpose of distinguishing the potential sites for tidal energy extraction which can be later verified by the field data.

As great multitude of tools and techniques are used to determine the amount of tidal resources and to quantify the resources available in different parts of the world, establishing a standard in extractable resource modelling can pave the way in promoting the adoption of tidal energy among the various stakeholders, as it can provide confidence in the amount of available resources. International Tidal Energy Working Group was thus consequently formed as a part of Ocean Energy Systems (OES), an International Energy Agency Initiative and various international research teams conduct extractable resource studies to share their results and methodology, and work towards creating a standard report for modelling in harnessing tidal energy. Thus, the main objective of this initiative is to develop a simulation guideline report of tidal energy resource modelling through a common case study with various factors along with code-to-code comparisons of various modelling strategies that exist in different parts of the models. It would also involve comparison of models with experimental data and also discussion on various assumptions made in models such

as seabed friction effects, wind driven forces etc.

The main goal of this workshop was to discuss and develop a standard methodology for modelling in harnessing tidal energy through study of various factors which affects tidal modelling of an ocean site and the various underlying assumptions behind the simulations. The working group was formed as an international team of tidal energy researchers towards a joint exercise effort concentrating on the accurate modelling and reporting the guidelines towards tidal energy resources.

2. Scope and Objectives

Scope of work of this workshop are as follows:

- Mapping the tidal resource, using ocean models, for potential case studies globally.
- Ocean condition characterization, with observation data and coupled wave-tide models, to inform resilience and yield optimization.
- Predictions of power for assessment of suitability to end users through Techno economics.

The objectives of this report are as follows:

- To highlight the various ocean modelling strategies adopted by international experts all over the globe.
- To highlight the various issues faced by experts during tidal resource modelling of sites.
- To compare the results of various ocean models for common temperate and tropical case studies using common input and validation data addressing the solutions to various concerns in tidal resource modelling.
- To understand the methods of representation of tidal model results as per EMEC guidelines.
- To introduce the various input databases available for ocean modelling (Annex A).
- To highlight the various ocean models available in commercial market as well as in open source (Annex B).

3. Ocean Modelling Strategies

To analyse the hydrokinetic power of tidal currents is important to realize that this power has a direct relationship with the velocities involved. Specifically, the tidal current power per m^2 is defined as

$$P = \frac{1}{2}\rho V^3 \quad (1)$$

where,

P is the hydrokinetic power (W/m^2)

v is the velocity of the current (m/s)

ρ is the water density (kg/m^3)

The energetic potential is defined as

$$E = \int P\,dt = \int \frac{1}{2}\rho V^3\,dt \quad (2)$$

where,

E is the energetic potential calculated in a certain period (Wh/m^2)

Both power and energy depend on the cube of the current speed. They are greatly boosted by any small increment in the available velocity. The variability of the sea water density is much lower than the current speed. Therefore, the velocity can be considered as the only relevant factor for estimating the potential of the currents.

To evaluate the feasibility of a possible energy installation based on devices obtaining energy from tidal currents, the first issue is to know the energetic potential (of tidal currents) in the site of study. This usually implies the development of an ocean model using a specific tool (or code) validated by field measurements.

There are one-, two-, and three-dimensional commercial codes, widely used to obtain ocean models for different purposes, usually sediment and pollutants transport and flood studies (in rivers, estuaries, and coastal regions). If they can be easily adapted to calculate tidal energy potential, they could be a very useful tool, as they are contrasted and have been used for many years, with an important user´s and developer´s communities and, therefore, experience and support. Recently a study has been published analysing the applicability of these codes to calculate the tidal range energy potential (Neill et al., 2018). This application is relatively simple because

it only involves the sea level changes and does not have to take into account the machinery. However, the studies concerning the energy potential of tidal currents are relatively scarce and with a wide range in depth and quality. Preliminary studies do not consider the variations of the velocity field due to the presence of turbines, while in the most complete their presence is considered through different approaches (Bryden & Couch, 2006; Vennell et al., 2015).

1D software tools are a simplified option, suitable when the tidal currents have a predominant direction. The information needed to elaborate the geometrical model is small (transversal sections separated a certain distance) and requires few computational resources. 2D software tools are more suitable than 1D in cases of abrupt variations of the geometry (narrowing's, curves, etc.), because the tidal currents are highly bidimensional. They require an increased computational time and more accurate information to elaborate the geometrical models. Nowadays, the three dimensional (3D) numerical models provide the most realistic analysis of the flow behaviour, however, they involve the highest need of computational resources details of the geometry.

Regarding 1D and 2D numerical codes, the most important simplification is that these codes solve a depth-averaged form of the differential Shallow Water Equations also referred as Saint–Venant equations. These equations are obtained from the continuity and momentum Reynolds-Averaged Navier–Stokes (RANS) equations, integrating them over the water depth, assuming incompressible flow and hydrostatic pressure distribution, and thus disregarding the effect of the vertical length scale, as it is much smaller than the horizontal one. Additionally, the turbulence stresses are calculated with Boussinesq assumption, with different eddy viscosity approaches depending on the code. This allows obtaining horizontal depth-averaged velocities and the free-surface height in large domains with affordable computational costs.

These codes use the Saint–Venant equations in their conservative form, which has great advantages when considering solving schemes that allow discontinuities in the solutions (wave fronts or hydraulic jumps). The final conservative equations in vector form are.

$$\frac{\partial U}{\partial t} = \nabla\big(F(U) - N(U)\big) = S \tag{3}$$

where,

U = (h, hU, hV) is the vector of depth-averaged flow variables; h is the water depth; and U and V are the velocities in the horizontal plane

F(U) is the tensor including spatial variations of the flow variables (or convective terms)

N(U) is the tensor including the turbulent stresses (or diffusive terms)

S is the tensor of source terms; it includes the effects of bed slope and bottom friction and, depending on the code, the wind stress and Coriolis force

Regarding 3D codes, they solve the full Navier–Stokes equations (continuity and momentum conservation equations) in 3D geometries for incompressible flow with simplifications due to the usually large zones they are applied to. The most relevant simplification is not considering inertial accelerations in the vertical momentum equation and, therefore, assuming a hydrostatic pressure distribution. The resulting equations are called three-dimensional shallow water equations (3D-SW)(Casulli & Walters, 2000). However, for flows where depth cannot be assumed to be much smaller than the horizontal length scale, some models include a nonhydrostatic option (Casulli & Walters, 2000). To consider the turbulence effects, the equations are solved (in most cases) with averaged variables, the simplified Reynolds-Averaged Navier–Stokes equations, and completed with turbulent models based on Boussinesq' s hypothesis. The codes use different numerical schemes to solve the differential equations. They are based on different spatial discretization methodologies - finite volumes (FV), finite differences (FD) or finite elements (FE)–applied over a mesh dividing the domain into cells. Usually, the codes give the user the possibility of defining the mesh features in the domain: zones of different mesh characteristics, number, geometry, and size of the cells, etc. The decision is a compromise between the accuracy and the resolution time. The numerical schemes imply the use of a resolution technique—explicit or implicit—and different order discretization of the derivatives terms–first- or second order. Additionally, each scheme implements its wetting and drying algorithm, eliminating or including different zones in the calculation while determining the position of the free surface.

3.1 1-Dimensional models

The 1D models are the simplest, but also the least accurate ones. They are valid when the tidal flow is one-dimensional or where the direction of the water movement is

aligned to the centre line of the tidal channel. They solve one-dimensional Saint–Venant unsteady equations (in our case, the tides fluctuations require the unsteady terms). The results obtained with these models are the water depth and the cross-section mean velocity. It is common that these codes do not implement turbulence effects nor Coriolis forces. Additionally, the numerical schemes are mainly implicit FD, but each scheme has its own resolution methods for discontinuities in the flow. In these simulations, the computational effort is typically very low. They are considered useful for a first approach of tidal energy evaluation but, usually, the energetic potential calculation is not very accurate because it does not take into account the section differences.

3.2 2-Dimensional models

These models are applied to flows with more complex geometries, or when there are some strong variations of the velocity in the cross-section (recirculation, vortex, gradients, etc.). They can obtain a more accurate description of the velocity field and, therefore, a better estimation of the energy potential. For unsteady cases, like tidal flows, the 2D codes solve the full (two-dimensional) Saint–Venant equations. The results obtained are the water depth and depth-averaged velocities. Basically, all of them address the turbulence with Boussinesq eddy viscosity approach, giving the user the choice of different turbulent models. Furthermore, these 2D codes implement high resolution schemes to obtain accurate results in cases of flow discontinuities (wave front or hydraulic jumps). It is very popular the high precision FV explicit schemes based on Riemann solvers(Roe, 1981; Yadav, n.d.). It is also common (when they are an evolution of finite differences 1D codes) the use of resolution schemes based on the FD Alternating Direction Implicit (ADI) methodologies. As it has been mentioned earlier, 1D codes are rather limited for the calculation of the energy extracted by the current turbines. The 2D codes, however, are more suitable. None of them has an explicit module to handle current turbines, but they can be simulated using different approaches depending on the capabilities of the software, for example, as an increased bottom roughness.

3.3 3-Dimensional Models

3D models allow the definition of the complex numerical meshes sometimes needed due to the irregular surface geometry and depth of the coast. This characteristic is not

so necessary to model the rivers, but it can be very useful for the analysis of the energy extraction with hydrokinetic turbines. All the codes divide the geometry in two parts: water surface and depth. For the water surface, the solutions are based on the use of structured orthogonal–curvilinear or unstructured meshes. For the depth or vertical dimension, the strategy proposed by the models is to divide the 3D geometry in different layers at diverse water depths, with two variations: Z-coordinate or σ-coordinate. In the first one, the domain is divided in horizontal layers with fixed thickness. When calculating, the code determines the number of active layers depending on the water level. The second one, the σ -coordinate, divides the depth in a constant number of layers with variable thickness, adapted to the bed shape and the water level. These codes usually consider the turbulence by the Reynolds averaging of the Navier–Stokes equations (RANS), where Reynolds stresses are calculated using the Boussinesq´ s hypothesis (eddy viscosity concept). The different turbulence models are basically the diverse implementations of these calculations. Another and more direct approach are the large eddy simulation (LES). In this case, the effect of the turbulence is directly calculated for the larger eddies, while the dissipation of the smaller ones is considered through a subscale turbulence model. This method should obtain a more accurate result, but it requires a rather finned mesh and quite large computational resources.

4. Common issues in Tidal resource Modelling

Some of the common issues in tidal resource modelling of a site are as follows:

- Wind - Wave generation: Dominant wave types in terms of wave period/frequency and amplitude. Classification and effects of damping parameters
- Wave-current interaction and wave breaking to address the following:
  - Resultant water surface elevation
  - Resultant direction of current
  - Basis for coupling between current and waves
  - Influence on tidal energy
- Modelling of the seabed and coastline depicting the quality of the sand in terms of its constituents for addressing the friction/drag force generated over the water flow.

- Effects of salinity and temperature in resultant tidal velocity and direction both qualitatively and quantitatively.
- Coupling of ocean model with CFD models for turbine site match making
- Better methods of validating the ocean models.
- Available open source ADCP and Tide gauges data for validation of tidal models.
- Hydrodynamic impacts of tidal current generation.
- Coupled 3d tide wave ocean models to parameterize realistic conditions to inform device scale studies.
- Parametrization of tidal turbines in the ocean model.
- Estimation of firm power and highest yield of tidal turbines as part of deterministic tidal resource prediction.
- Inclusion of technoeconomic aspects and environmental effects.
- Effects of power extraction on water level, current speed and residual current.
- Shortcomings of analytical models - Analytical models neglects turbulent mixing and 3d structure flow and thus underestimates the turbine efficiency

5. Temperate Waters Case Study

Referring to EMEC standard, for the purpose of investigating potential sites where tidal energy converters can be deployed, studies were conducted from regional assessments to various phases of site assessments (from initial examination to detailed examination). At the initial stage, we planned to determine a suitable site for temperate case study. The details of chosen site conditions for modelling study are as follows:

- Case study site: Alderney race close to Cherbourg, France
- Macro level domain dimension: 500 km by 300 km
- Source of bathymetry: ETOPO, GEBCO or SRTM
- Source of tide height input: TPXO8/OTPS, FES, DTU Global Tidal Model, different models have their own consideration in how they resolve in shallow and deep waters.
- Coastline data source: Global Self-Consistent, Hierarchical High-Resolution Geography Database (GSHHS)
- Ocean models: 2D or 3D models

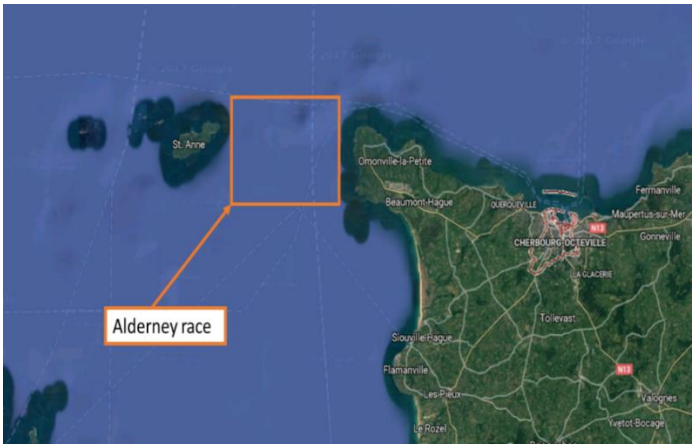

Figure 1: *Case study – Alderney Race*

After comparison with various modelling strategies, we came with top 5 different methods as shown in Figure 2 below. Method 1 is based on 2D RANS equation based Finite Element model, Method 2 is based on 3D baroclinic Nonlinear Shallow water equations based Finite Element model, Method 3 is based on 3D baroclinic Arakawa B-grid Shallow water equations with the hydrostatic and Boussinesq approximations model, Method 4 is based on 2D depth average unsteady shallow water equation based finite difference model and Method 5 is based on 2D depth average Shallow water equations based finite element model. International teams were grouped and were asked to simulate the ocean models based on these methods for comparison study.

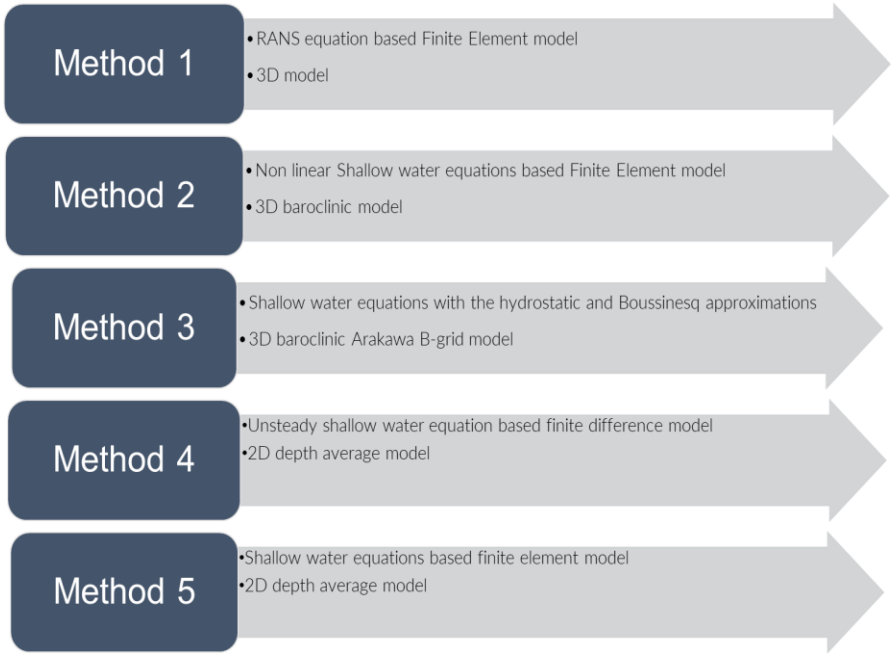

Figure 2: *Selected five methods.*

5.1 Method 1

The tide propagation in the Alderney Race was simulated with an Ocean model, which solves the free-surface RANS equations using a finite element method (Hervouet, 2007). The turbulence is modelled with k-ε (horizontal and vertical directions). The continuity and momentum equations take the following form:

$$\frac{\partial u}{\partial x}+\frac{\partial v}{\partial y}+\frac{\partial w}{\partial z}=0$$
$$\frac{\partial u}{\partial t}+u\frac{\partial u}{\partial x}+v\frac{\partial u}{\partial y}+w\frac{\partial u}{\partial z}=\frac{-1}{\rho}\frac{\partial p}{\partial x}+\nu\Delta u+f_x$$
$$\frac{\partial v}{\partial t}+u\frac{\partial v}{\partial x}+v\frac{\partial v}{\partial y}+w\frac{\partial v}{\partial z}=\frac{-1}{\rho}\frac{\partial p}{\partial y}+\nu\Delta v+f_y$$
$$\frac{\partial w}{\partial t}+u\frac{\partial w}{\partial x}+v\frac{\partial w}{\partial y}+w\frac{\partial w}{\partial z}=\frac{-1}{\rho}\frac{\partial p}{\partial z}-g+\nu\Delta w+f_z$$

where x and y are the geographic coordinates, z is the vertical coordinate, u, v and w are the three components of the velocity field, t is the time, g is the gravity acceleration (g = 9.81 m/s^2), ν is the kinematic viscosity (molecular and turbulent viscosity), f_x, f_y and f_z are the source terms (bottom friction, Coriolis force) and ρ is the water density (ρ = 1025 kg/m^3).

The computation domain covers the English Channel. The mesh density is imposed using cell sizes ranging from 10 km to 100 m. The horizontal mesh contains 240,807 nodes and the domain is discretized vertically using 40 equally spaced horizontal planes (sigma-transformation). The bathymetric data come from a Digital Elevation Model (DEM) provided by SHOM (*MNT Bathymétrique de Façade Atlantique (Projet Homonim) NM*, n.d.). The resolution of the DEM is 0.001° (≈111 m). The model time step is 10 s. Conditions along the Western and Northern sea boundaries are provided by the TPXO European Shelf 2008 database (G. Egbert et al., 2010). The bottom shear stress $\overrightarrow{\tau_b}$ is computed with the following friction law, which accounts for the seabed roughness:

$$\overrightarrow{\tau_b}=\rho C_b\|\vec{U}\|\vec{U} \qquad \text{with } C_b=\left(\frac{\kappa}{ln\,(H/ez_0)}\right)^2$$

where $\|\vec{U}\|$ is the magnitude of the depth-averaged horizontal current, $C_b$is the friction coefficient, $\kappa = 0.4$ is the von Karman constant, H is the water depth and z_0 is the bottom roughness defined as the height above the seabed where the fluid velocity is nil. The roughness parameterization is based on a sedimentological cartography established by SHOM.

The hydrodynamic model of the Alderney Race is assessed against ADCP measurements provided by OpenHydro. This dataset gathers measurements acquired by 5 ADCPs deployed simultaneously around the Alderney Island. The height of the vertical cells is 2 m and the ADCP sampling frequency is 1 Hz. The validation period covers neap and spring tides. It extends from August, the 6th in 2014 at 00:00 (UT) to August, the 12th at 00:00 (UT). The model is run 24 h before the beginning of the validation period to allow the model spin up from the initial conditions. The meteorological forcing (wind and pressure) and the wave effect are not integrated assuming that the hydrodynamics of the Alderney Race is mostly controlled by the tide (G. Egbert et al., 2010).

The model validation is based on the magnitude and direction of the horizontal velocities. Parameters used for the assessment of model's predictions are the mean error ME, the mean relative error MRE and the index of agreement IA. The indicator errors are listed in Table 1. An overall good agreement is found between observations and model predictions either in terms of magnitude or direction. As regards the velocity magnitude, the mean index of agreement is 0.983, which indicates very good model performances.

Table 1: Performance indicators for the depth-averaged velocities

ADCP n°	ME Norm[m/s]	MRE Norm[%]	IA Norm[ ]	ME Dir [°]
1	-0.13	-8	0.962	-7
2	-0.01	-1	0.986	-6
3	0.01	1	0.990	10
4	0.01	-1	0.989	-4
5	-0.00	-0	0.990	2

5.2 Method 2

For this method, the nonlinear shallow water equations were solved with a finite element discretization that uses piecewise-linear, discontinuous function spaces for both velocity and free surface elevation. A Manning formulation is used to describe the bed friction term. Unstructured triangular meshes were generated using qmesh, with the base case mesh comprising of 60,658 elements. Marine Digimap bathymetry at a resolution of 30m is used, with coastlines taken from the Global Self-consistent, Hierarchical, and High-Resolution Geography Database (GSHHG) (*GSHHG - A Global Self-Consistent, Hierarchical, High-Resolution Geography Database*, n.d.).

At open boundaries the free surface elevation is specified using the leading eight tidal constituents from the TPXO European Shelf 2008 database (*OSU Tidal Data Inversion*, n.d.). The horizontal kinematic viscosity is set to a value of 10 m^2/s throughout the domain. To aid stability with the imposition of boundary conditions a "sponge region", ramping this value up to 1000 m^2/s over a region spanning 50km from the open boundaries, is utilized.

Simulations are spun up for five days where and then for a further 30 days to allow harmonic analysis to be performed. A time step size of 100 seconds is used. Results are then assessed against a number of tide gauges spread across the domain. For the bottom friction value initially a uniform Manning's *n* value of 0.023 is used.

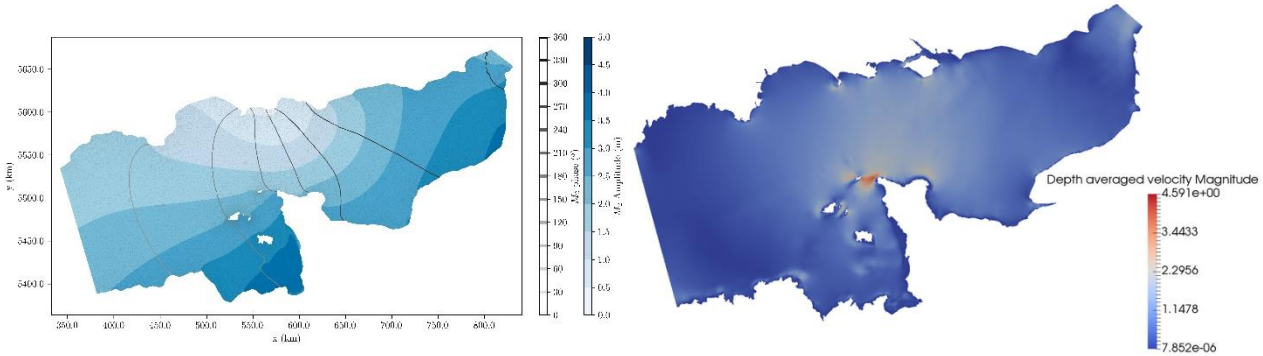

Figure 3: *the left frame shows a co-tidal chart for the M2 constituent amplitude and phase in the case of a simplified coastline. The right frame shows a snapshot of the depth-averaged velocity field in the case of a higher fidelity coastline.*

In (Goss et al., n.d.) a sensitivity study to mesh, bathymetry and coastline resolution is conducted. Figure 3 shows some example results for M2 elevation and instantaneous velocity field. None of these simple sensitivity/calibration studies were

found to easily yield substantially improved simulation results. Instead the adjoint capability available in Thetis was used to perform an optimal parameter estimation study. 32 tide gauges evenly spread over the domain were selected and a misfit function was defined in terms of the difference in the model elevation time series and corresponding series reconstructed from the harmonics at the tide gauges. This was done in order to limit the simulation period to 24 hours rather than the longer period that would be required to define the misfit in terms of harmonics. At each optimization iteration a forward model and adjoint calculation were performed, yielding the sensitivity (derivative) of the misfit to the Manning's *n* field. This was then used within a gradient-based optimization algorithm to update the Manning's *n* field, which was constrained to lie within the range 0.005 – 1. The updated variable friction field was then used within a longer simulation that allowed harmonics to be computed and a reduction in the normalized root mean square error in the M2 amplitudes over the calibrated 32 tide gauges reduced from 0.166 with the original uniform Manning's *n* field to 0.052 with the calibrated field. Ongoing work is seeking to address the clear issue of this being an under-constrained optimization problem by considering the use of regularization terms in the definition of the optimization functional, and by partitioning the seabed into a finite number of categories depending on seabed type and assuming a uniform drag value within each rather than attempting to optimize for a completely variable drag field. The issue of optimizing arrays on either side of the Alderney Race, and the impact of competition/collaboration effects is considered in (*Competition Effects between Nearby Tidal Turbine Arrays - Optimal Design for the Alderney Race*, n.d.).

5.3 Method 3

The hydrodynamics were generated by the ocean model (*An s Coordinate Density Evolving Model of the Northwest European Continental Shelf: 1. Model Description and Density Structure - Holt - 2001 - Journal of Geophysical Research: Oceans - Wiley Online Library*, n.d.), formulated in spherical polar coordinates and using 20 terrain following (sigma) layers in the vertical. The ocean model was formulated on the Arakawa B-grid, hence the Coriolis term is calculated without averaging (unlike the Arakawa C-grid where considerable averaging is required). It has been demonstrated that this grid formulation is important when considering the influence of Coriolis on sand bank formation, particularly evident when modelling idealized headlands (Neill,

2008)[24]. Neglecting the baroclinic terms and barotropic meteorological effects (e.g., wind stress and atmospheric pressure), the depth-mean equations of motion are (*An s Coordinate Density Evolving Model of the Northwest European Continental Shelf: 1. Model Description and Density Structure - Holt - 2001 - Journal of Geophysical Research: Oceans - Wiley Online Library*, n.d.)

$$\frac{\partial \bar{u}}{\partial t} = f\bar{v} - \frac{g}{R\cos\emptyset}\frac{\partial \zeta}{\partial \chi} - \frac{F_B}{H} + NL_\chi$$

and

$$\frac{\partial \bar{v}}{\partial t} = f\bar{u} - \frac{g}{R}\frac{\partial \zeta}{\partial \phi} - \frac{G_B}{H} + NL_\phi$$

where $\bar{u}$ and $\bar{v}$ are the depth-averaged eastward and northward velocities, respectively, ζ is water surface elevation relative to mean sea level (MSL), H = h + ζ is total water depth (where h is water depth relative to MSL), χ and ϕ are the eastwards and northwards coordinates, respectively, f = 2Ω sin(ϕ) is the Coriolis parameter (where Ω = 7.27 x10^{-5} s^{-1} is the angular velocity of the Earth), R is the radius of the Earth, g is gravitational acceleration, NL χ and NL ϕ are the nonlinear terms, and F_B and G_B are, respectively, the eastward and northward components of bed shear stress, calculated from

$$(F_B, G_B) = C_D\,(u_B, v_B)\sqrt{u_B^2 + v_B^2}$$

where u_B and v_B are the near-bed velocities, defined at a height δ above the bed, and C_D is the drag coefficient (based on an assumed logarithmic velocity profile)

$$C_D = \left(\frac{k}{\ln(\delta/z_o)}\right)^2,\ C_D \geq 0.005$$

where k = 0.41 is Von Karman's constant and z_0 is the roughness length. For turbulence closure, ocean model used the Mellore – Yamadae – Galperin level 2.5 scheme (*A Hierarchy of Turbulence Closure Models for Planetary Boundary Layers in: Journal of the Atmospheric Sciences Volume 31 Issue 7 (1974)*, n.d.; Galperin et al., 1988). Boundary conditions required for ocean model were elevation and the normal component of velocity. After spin up, output from the hydrodynamic model was stored for each model cell every 15 min until completion of the simulation.

Bathymetry for the study region was digitised from Admiralty Charts 60, 2669 and 3653, corrected for mean sea level, and interpolated onto a model grid with a horizontal

resolution of approximately 150 m. The entire model domain (Fig. 4) incorporates a much larger area than the Alderney Race (approximately 55 km x 45 km) in order to eliminate boundary effects and simulate far-field impacts.

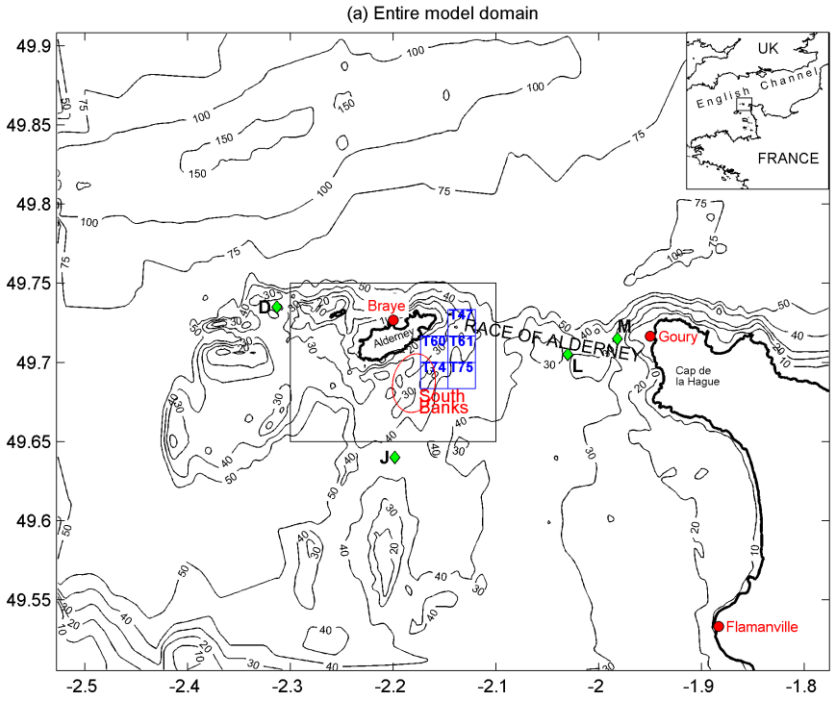

Figure 4 *shows extent of model domain (55x45 km) and validation stations (red=elevations, green=velocity)*

The boundary conditions were extracted from a larger area model of the northwest European shelf seas which has a resolution of $1/6^0$ longitude x $1/9^0$ latitude [40]. The ocean model was applied to the Alderney model grid over a spring-neap cycle, using the dominant semi-diurnal tidal constituents, M2 (lunar) and S2 (solar), as boundary conditions. The model of the Alderney region was successfully validated in terms of the magnitude and phase of the M2 and S2 elevations at three stations taken from Admiralty Tide Tables. The modelled tidal currents were also compared with the magnitude and direction of tidal currents at the location of four tidal diamonds taken from Admiralty Chart 3653. Although the magnitude of the peak tidal currents in the immediate vicinity of Alderney (tidal diamonds D and J) were on average within 5% of observed values, peak velocities in the eastern part of the Alderney Race (tidal diamonds L and M) were consistently over-predicted by an average of 16%. However, the simulated peak current directions were accurate to within an average of 9^0 across all locations.

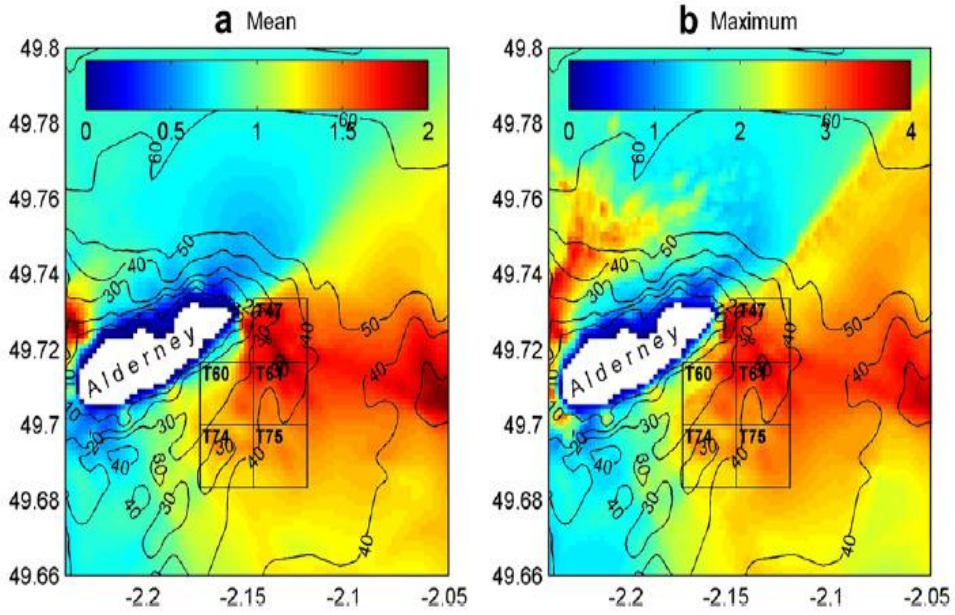

Figure 5: (a) mean and (b) maximum magnitude of velocity (in m/s) over a spring-neap cycle

5.4 Method 4

In the present study, the rectilinear grid was used to simulate the hydrodynamics around the Alderney race, France. The study domain was discretized into a constant size of 100m x 100m grid cells, which allowed for a much more accurate representation of the shorelines and bathymetry. The bathymetric data for the region was obtained from the General Bathymetric Chart of the Ocean (GEBCO)(Kapoor, 1981), which were interpolated onto the computational domain of the model by using the interpolation tool. The open boundary of the model was forced with time-varying tidal elevation as a form of tidal constituents extracted from TPXO 7.2 Global Inverse Tidal Model(*OSU Tidal Data Inversion*, n.d.). Finally, the model was run with a selected suitable time step that was satisfied with the Courant number criteria. The simulated result was compared with literature-based current data, and it shows good agreement. After the successful validation, the potential power density maps were derived from the tidal power density equation. The ocean model predicted with a root mean square error of less than 10 %.

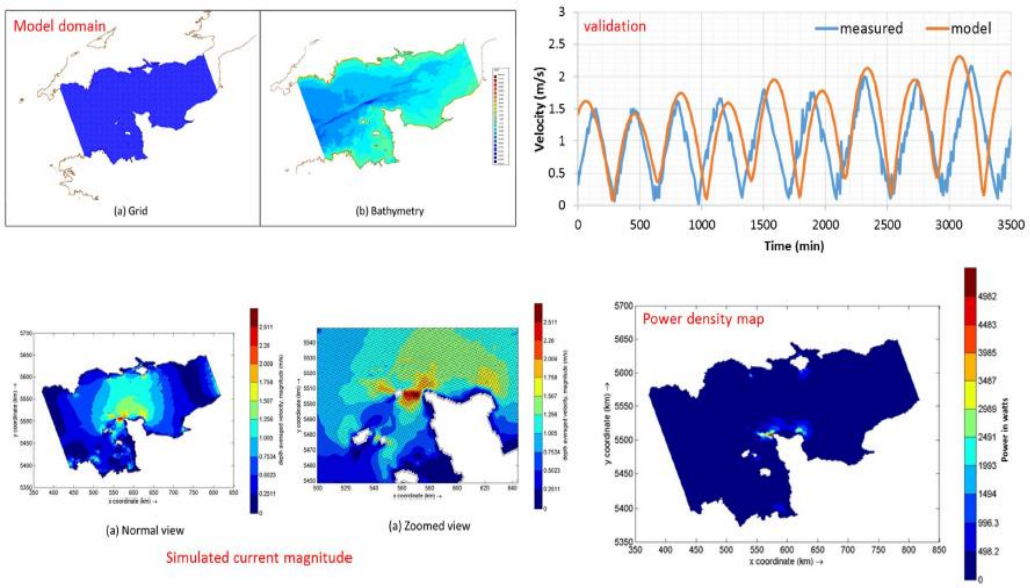

Figure 6: Modelling of tidal Stream Energy in the Alderney race

5.5 Method 5

The described ocean model consists of ocean boundaries, coastlines and islands along the English Channel. The domain size is around 500 km to 265 km as shown in Figure 7. The model was forced at the ocean boundary with K1, K2, M2, N2, O1, P1, Q1 and S2 tidal constituents. The tidal constituents were predicted using LeProvost Tidal Database (Le Provost et al., 1994).

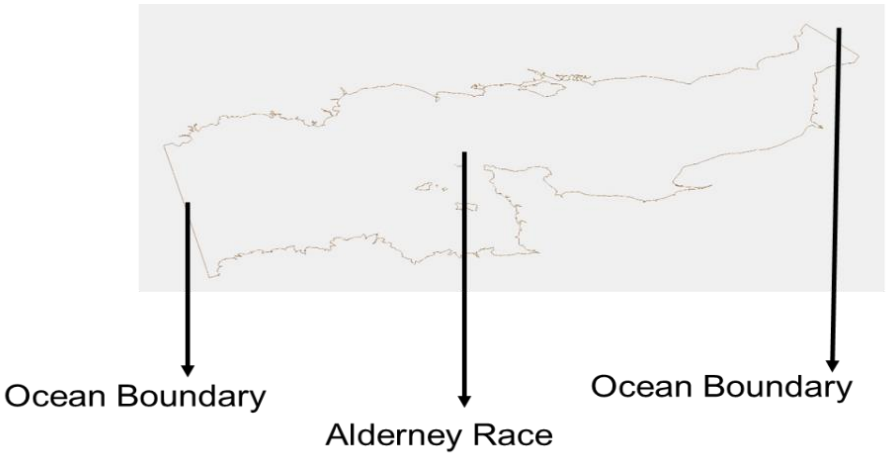

Figure 7: Model Description

An unstructured mesh grid of about 95,674 elements and 50,955 nodes were used for this model. Coastline data and bathymetry data are the input data required for the model. Coastline data for the described model was obtained from Global Self-consistent, Hierarchical, and High Resolution Geography Database (GSHHG) (*GSHHG - A Global Self-Consistent, Hierarchical, High-Resolution Geography Database*, n.d.) which was jointly developed and maintained by University of Hawai'I and National Oceanic and Atmospheric Administration (NOAA) Geosciences Lab, National Ocean Service, Silver Spring, MD. GSHHG coastline data is 1 minute arc gridded resolution data. Bathymetry data for the model was obtained from Generic Bathymetry Charts of the Ocean (GEBCO) (Kapoor, 1981) which was provided by British Oceanographic Data Centre (BODC) and it is a 30 second arc gridded data. The friction coefficient setup in the model is a quadratic varying friction coefficient along the depth profile of the nodes with a starting value of 0.005.

Simulations were run for a time period of 30 days with 5 ramp days for a time step of 5 seconds. The velocity time series, depth profile and surface elevation data was obtained.

The depth average velocity profile obtained by the ADCIRC finite element hydrodynamic model depicted the water flow in the Alderney race over a certain time. The variation of the velocity in the region the Alderney race showed a maximum value of 3.5 m/s as shown in Figure 8. This high value of the water flow makes this site of the English Channel a suitable place for the harness of the tidal energy.

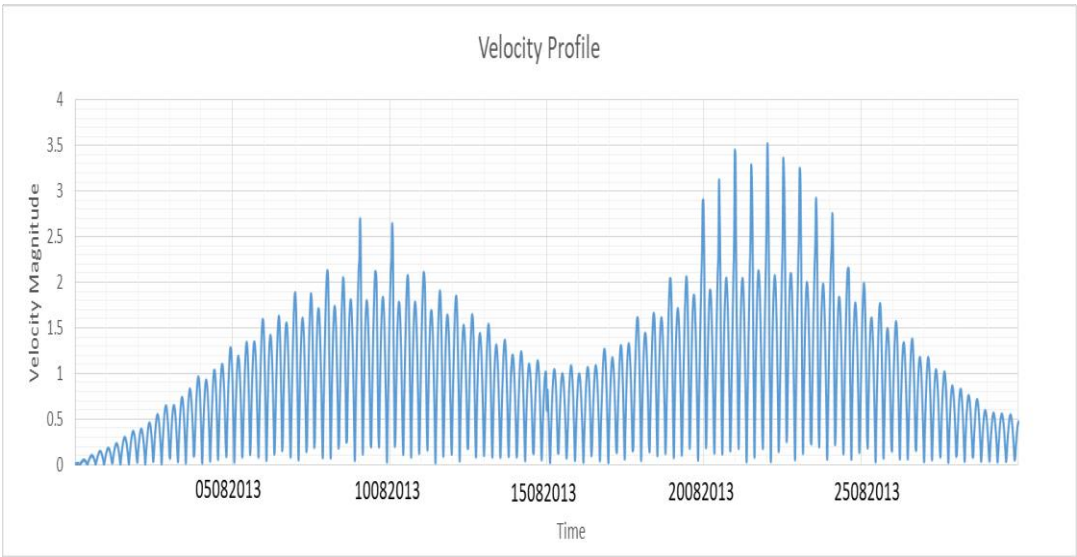

Figure 8: *Velocity Time series data*

As an estimate of the extractable tidal energy from the site, the variation of the Average power density (kW/m^2.) with time is as shown in Figure 9. A maximum average power density of 16 kW/m^2 was obtained which shows the high potential of site in generating tidal energy.

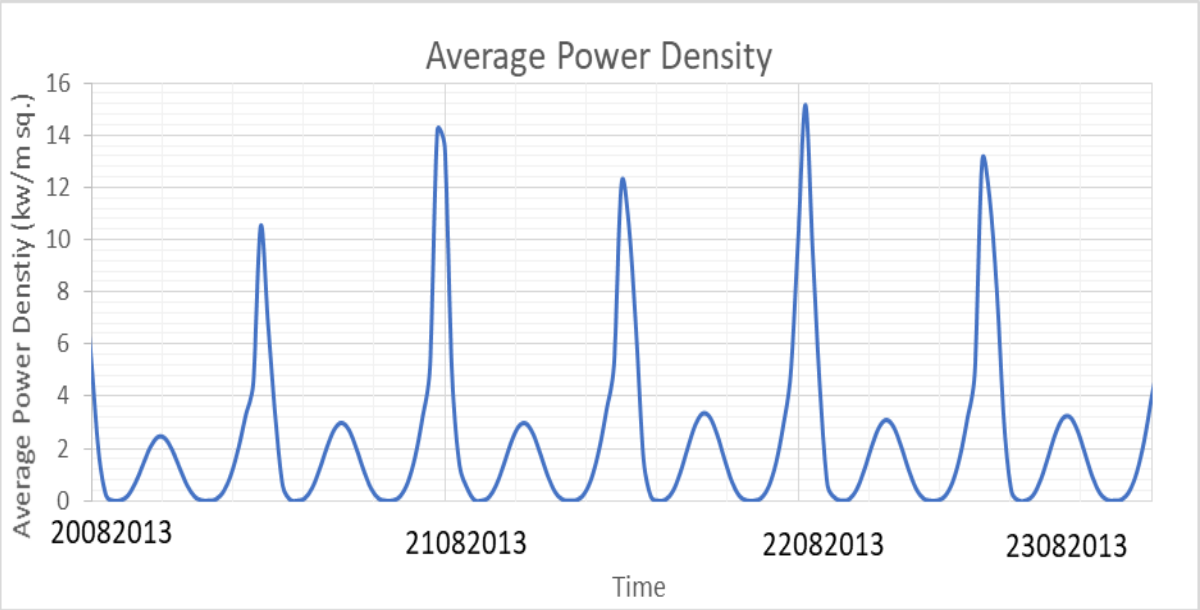

Figure 9: Predicted Average Power Density in Alderney Race

Further due to effect of tides, water surface level rises and fall and it is because of this rise and fall motion that the flow is induced in the surrounding water. Figure 10 shows the water surface elevation in the Alderney race. This rise and fall varies between -2m to 2m respectively with the variation of tide height of about 4 m.

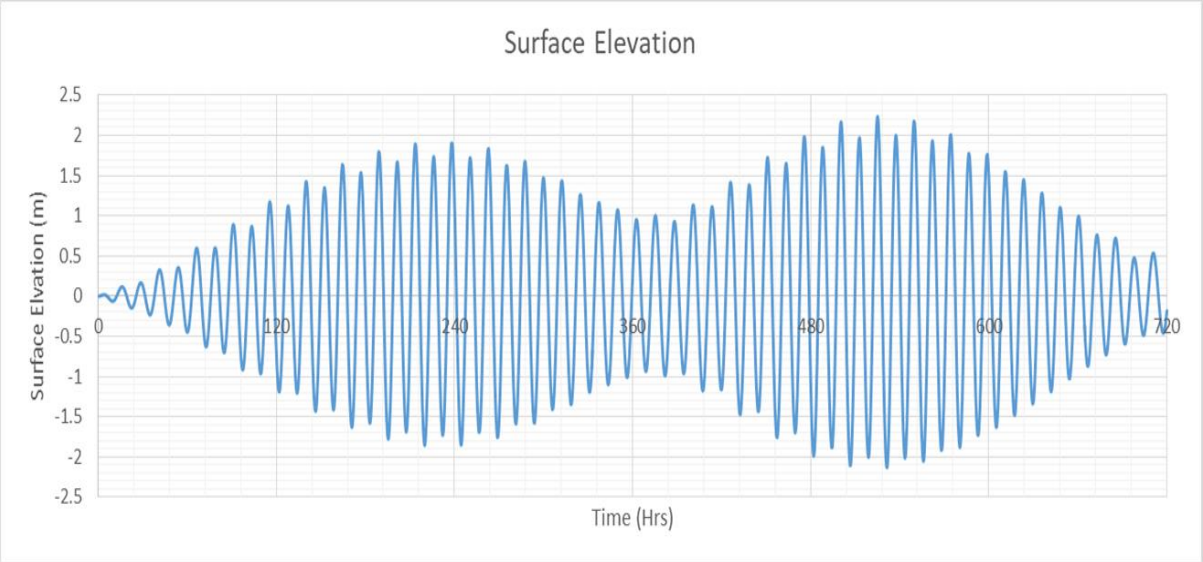

Figure 10: Predicted Surface elevation data of Alderney Race.

From the bathymetry data obtained from GEBCO, the maximum depth in the whole domain was about 166.47 m and the average depth in the Alderney race was about 40 m as shown in Figure 11.

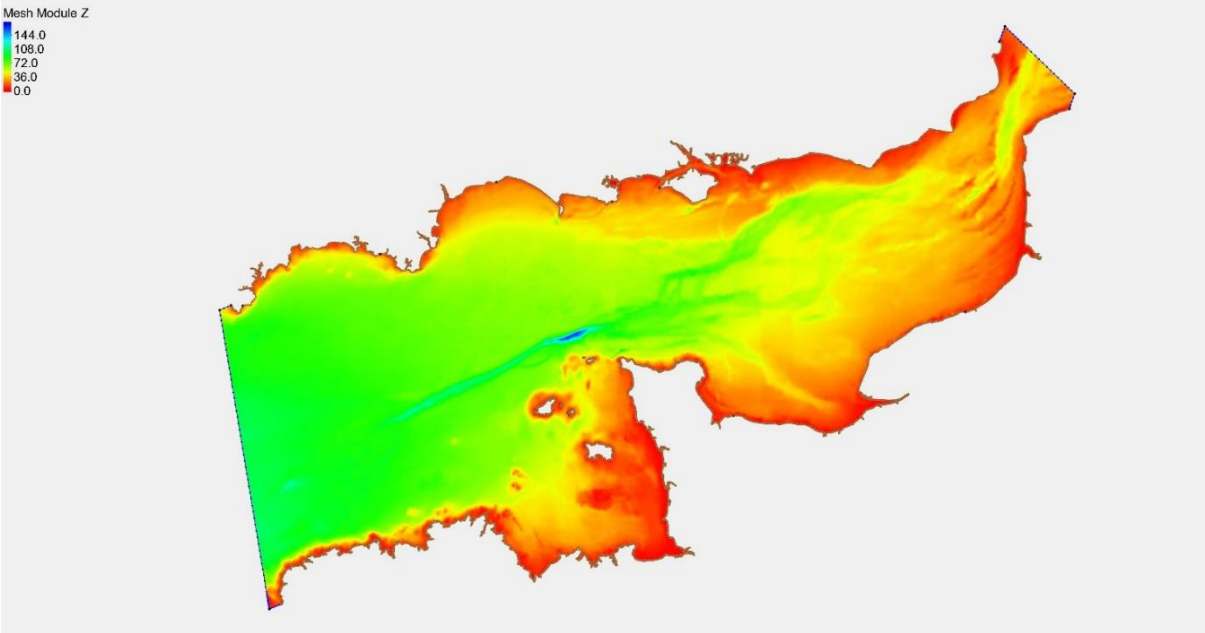

Figure 11: Depth Profile of Alderney Race

This present case study was used to illustrate the use of ADCIRC (an open source model) in Tidal energy modelling of Alderney race. ADCIRC, an open source model along with open source input data was used in order to help promoting Tidal Energy Modelling in OES countries which do not have enough information as well as licensed commercial models. The predicted maximum velocity in the Alderney race was about 3.5 m/s with average power density of about 16 kW/m^2 and the tidal height variation was about 4 m. The present prediction was well in line with other predicted models. The model has also been validated for few sites in various parts of South East Asia and was compared with its real time data obtained from ADCP deployed in various sites. The ocean model predicted with a root mean square error of about 5 - 10 %.

In overall, ocean models with various selected methods was simulated and tidal energy potential of the common case study of the Alderney race was determined. The Root Mean Square Error of all the models was less than 10 % which can be summarized as shown in Table 2.

Table 2: Comparison of Models

Description	**Method 1**	**Method 2**	**Method 3**	**Method 4**	**Method 5**
Model	RANS equation based Finite Element model	Nonlinear Shallow water equations based Finite Element model	Shallow water equations with the hydrostatic and Boussinesq approximations	Unsteady shallow water equation based finite difference model	Shallow water equations based finite element model
Bathymetry Data	Digital Elevation Model (DEM)	Digimap	Digitized from Admiralty Charts 60, 2669 and 3653	Satellite data	Satellite data
Coastline Data	Satellite data	Satellite data	Digitized from Admiralty Charts	Satellite data	Satellite data
Tidal constituents	European Shelf 2008	European Shelf 2008	NW European shelf seas	Global Inverse Tidal Model	Leprovost tidal database
Mesh	240,807 nodes	60,658 elements	-	-	95,674 elements
Number of days simulated	30 days	30 days	30 days	30 days	30 days
Effects of seabed friction	Yes	Yes	Yes	Yes	Yes

Effects of wind	No	No	No	Yes	No
RMSE	< 2 %	5 %	5 – 10 %	< 10 %	5 - 10 %

6. Tropical Waters Case Study

As a second case study, we planned to determine a suitable site for tropical case study. The details of chosen site conditions for modelling study are as follows:

- Case study site: Lombok straits, Indonesia
- Latitude: 8.2-8.6 N, Longitude: 115.10 -116.10E
- Source of bathymetry: ETOPO, GEBCO or SRTM
- Source of tidal input: TPXO8/OTPS, FES, Le Provost Tidal Database
- Coastline data source: Global Self-Consistent, Hierarchical High-Resolution Geography Database (GSHHG)
- Common ADCP validation data.

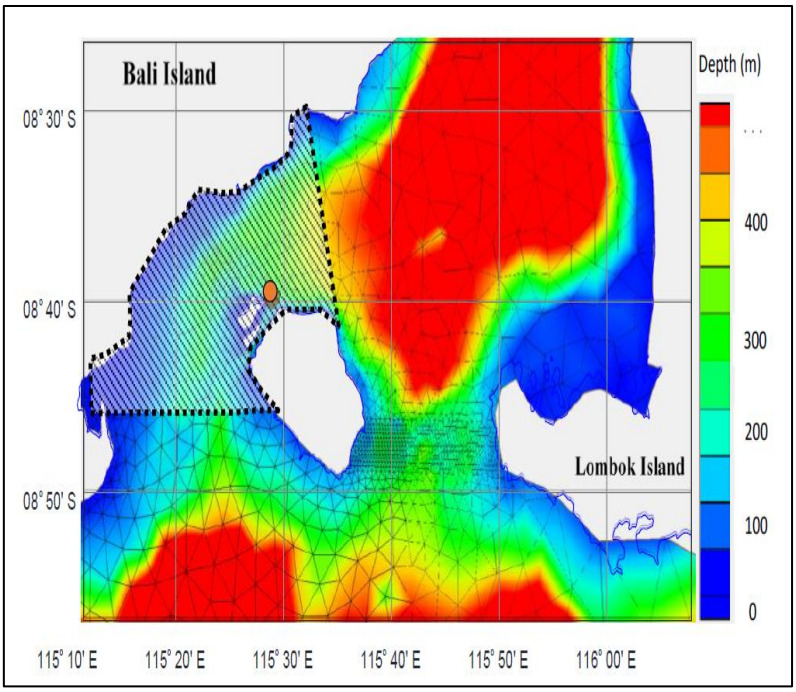

Figure 12: *Case study – Indonesia*

International teams were asked to simulate the case study based on their ocean models for comparison study.

6.1 Method 1

The simulation for tidal resources in this report is from (Adcock et al., 2013). The Discontinuous Galerkin version of Advance Circulation (DG-ADCIRC) Model was used to solve the Shallow Water Equations (SWEs) to model the tidal hydrodynamics. This model uses the GEBCO bathymetric data. However, Koropitan and Ikeda have shown this dataset to be inaccurate in the central and coastal regions in the Java Sea, and we also found this is to be the case. Hence, bathymetric chart data from DISHIDROS TNI-AL, a hydro-oceanographic Division of the Indonesian Navy, is also incorporated. Several bathymetric maps from DISHIDROS in the Java Sea, Banda Sea and Makassar Sea are combined as shown in Figure 13 in the region enclosed by the dotted line.

The model domain was set at far away from the interest location in Lombok Strait, following (Draper et al., 2014), (*Tidal Power Generation – A Review of Hydrodynamic Modelling - Thomas AA Adcock, Scott Draper, Takafumi Nishino, 2015*, n.d.) and (Le Provost et al., 1994). This set up was taken to ensure the interaction between the turbine existences in the simulation could be neglected.

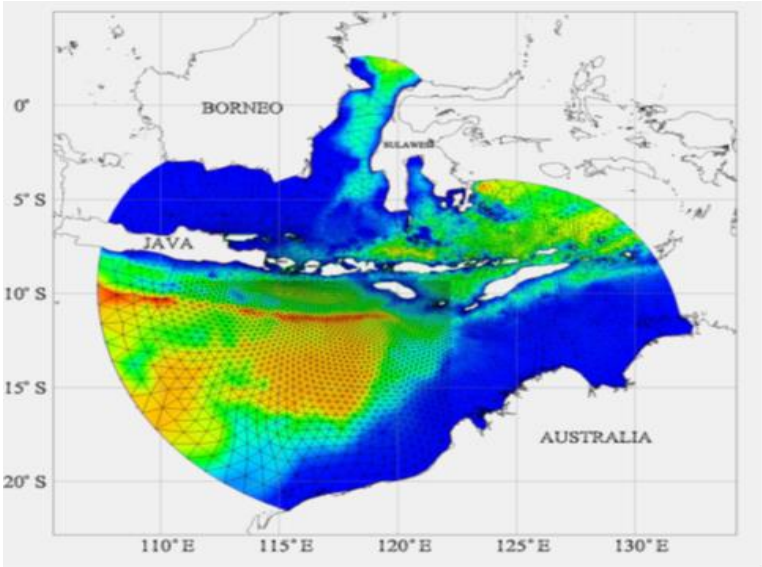

Figure 13: *Model domain with and mesh and bathymetry.*

The simulation was forced with thirteen tidal components applied at the boundaries, using data from the Le Provost model (Le Provost et al., 1994).This area is passed through by a thermohaline circulation from Pacific to the Indian Oceans (Gordon, 2005), this current known as Indonesian Through Flow (ITF). To mimic the ITF, a small

differential head at each boundary was applied. The mean elevations on Open Ocean boundaries are set as 0.0075 m, 0.01 m, 0.005 m and 0.000 m on boundaries ABCD respectively. For example, these head differences between the northern and southern boundaries, creates a flow in the area of Badung with a velocity ranging from 0.25-0.35 m/s. Because of the inclusion of the ITF as a residual current, the model is spun up for 2 days before the results from the following 60 days are recorded and harmonically analyzed for comparison with data.

The model was validated using several data sources. In addition to comparing with the tidal elevations, as is commonly used for validation, the model was validated with a co-tidal chart and with time series of tidal observations and an ADCP current measurement survey. The comparison of ADCP current measurements and the model results is presented in Fig. 14. Despite the fact that the model gives smaller velocity magnitudes, this comparison shows that model matches the velocity pattern quite well. Fig. 15 shows that the tidal elevations match better than the velocity.

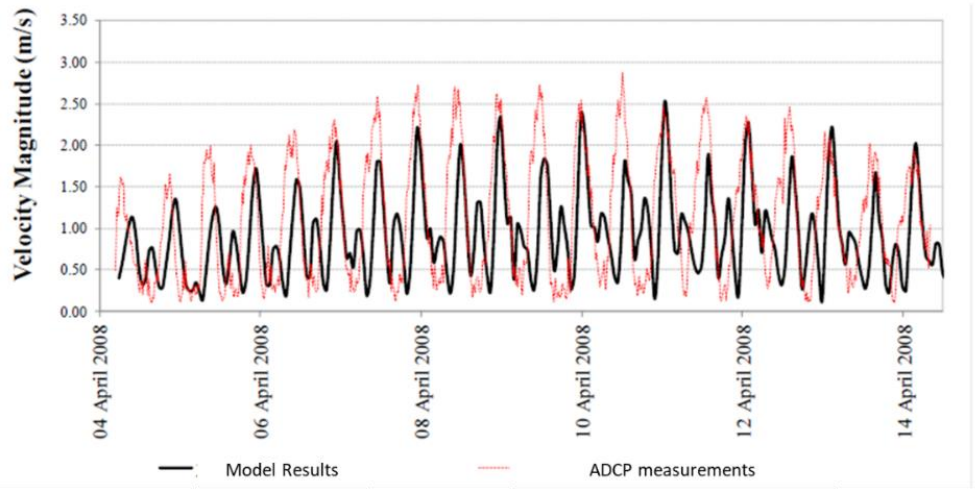

Figure 14: Comparison of current velocity from model and measurement using ADCP (mean from in several water depths). The ADCP data was conducted by (Kurniawan et al., 2021).

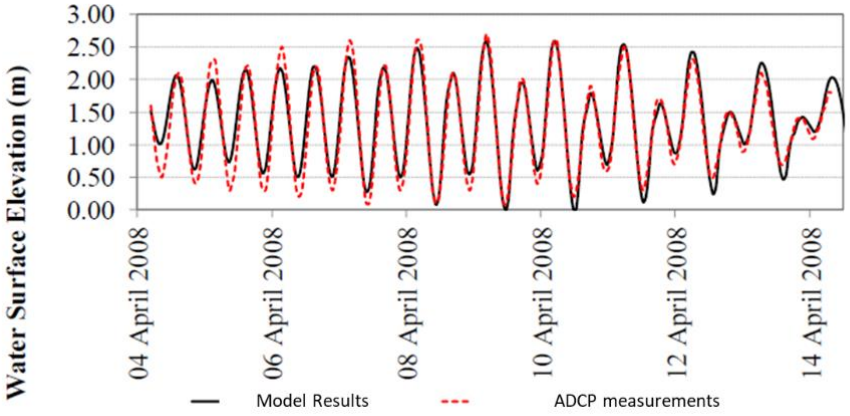

Figure 15: Comparison of model and tidal elevation observations that was obtained from (Kurniawan et al., 2021).

The potential tidal energy resources are assessed by installing a ~13.8km long turbine array at Badung (A), ~980m long at Toyopakeh (B) Strait and 25km long at Lombok (C) Strait (see Figure 16). In the analysis a fence of turbines occupies whole channel width in each strait. This simulation might not reflect the reality as we are aware that is impossible to occupy the entire cross section of this channel. The Lombok Strait (C) is an international shipping lane that known as ALKI.

Tidal energy resources are assessed here by Linear Momentum Actuator Disc Theory (LMADT) or we called this method as Houlsby-Whelan Model (*Assessment of Tidal Power Opportunities in Indonesian Waters - ORA - Oxford University Research Archive*, n.d.)[43]. This method was named this is called Houlsby-Whelan model here

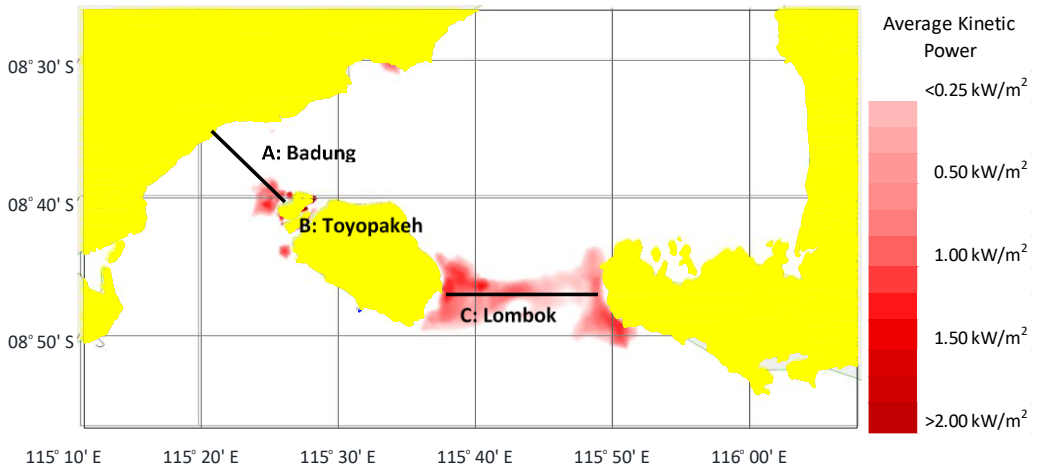

Figure 16: Potential areas for turbine arrays and kinetic power density as later discussed in 10.3. The result was taken from [36]

as the work has been done by(Houlsby et al., 2008; Houlsby & Vogel, 2016) and (WHELAN et al., 2009). The Power (*P*) removed from the flow in an open channel is calculated by:

$$P = \frac{1}{2}\rho u^3 B A_c C_p$$

where *u* is velocity of the tidal stream, B is blockage ratio, A_c the cross sectional area of the channel and C_p is a dimensionless power coefficient which is a function of the upstream Froude Number, the blockage ratio and the wake induction factor α_4. For further detail see (*Assessment of Tidal Power Opportunities in Indonesian Waters* -

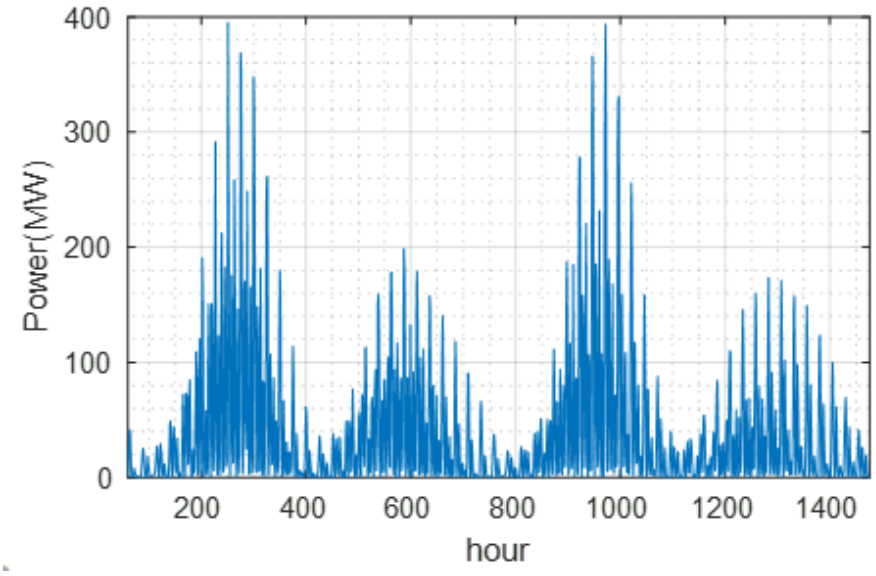

Figure: 17 Power Extraction of Individual Fences at Badung Strait (A) the result was taken from 36

ORA - Oxford University Research Archive, n.d.; Houlsby et al., 2008; Houlsby & Vogel, 2016; WHELAN et al., 2009).

In the assessment, three different wake coefficients (α_4) are applied to each array. An example of power extraction time series is presented in Figure 17. Average power extraction is calculated for each case and plotted against α_4. The optimum α_4 at which maximum power extraction is achieved is obtained by fitting a cubic spline through the data points. The entire assessment is carried out for two blockage ratios: B = 0.1 (low blockage) and B = 0.4 (high blockage).

The average resource at Badung is approximately ~39 MW while Toyopakeh is ~4.4 MW and Lombok is ~273 MW at low blockage ratio. Atlantis Resources Ltd. (Atlantis) and DCNS Energies promised to deliver 150 MW electricity from this site. It seems this can be achieved at low blockage from Lombok Strait. At high blockage, the resources increase significantly, and is about five to six times higher than for the low blockage case. In detail the resource in Badung is ~232 MW or almost six times higher, Toyopakeh is ~22 MW or about five times higher and Lombok is ~1.8 GW, more than six times higher than the resources at B = 0.1. These results show that the given sites are promising for tidal turbine implementation.

The simulation is also simulated the site-site interaction. The power extraction in a channel could affect the resources that could be extracted in other channel. This site-site interaction analyses have been studied by (Draper et al., 2014) and(Coles et al., 2017) in the Pentland Firth and Channel Islands. Similarly these studies we also found that the channel of Badung (A), Toyopakeh (B) and Lombok (C) could affect each other channel (see (Firdaus et al., 2019)for the detail).

6.2 Method 2

A three-dimensional, free surface, terrain-following numerical model that solves finite difference approximation of the Reynolds-averaged Navier-Stokes (RANS) equation using the hydrostatic and Boussinesq assumption with split-explicit time stepping algorithm (Walters, 2005) was used for the ocean model of Lombok straits, Indonesia. The entire domain was of 9102 sq kilometers with 123km in longitudinal direction and 74km in the latitudinal direction as shown in Figure 18.

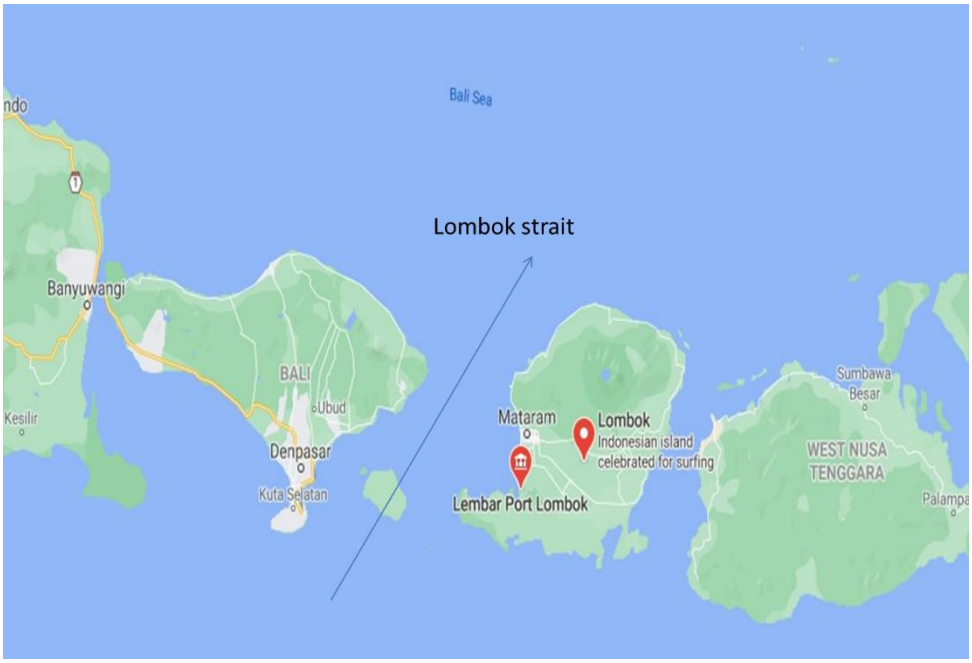

Figure 18: Model domain

The depths vary up to more than 2000m at certain points within this domain. The vertical levels have been divided into 15 equidistant levels for the entire depth and for computational purposes, the domain is itself forced with 7 vertical levels.

Bathymetry data for the model was obtained from Generic Bathymetry Charts of the Ocean (GEBCO) (Kapoor, 1981) which was provided by British Oceanographic Data Centre (BODC), and it is a 30 second arc gridded data. However, Koropitan and Ikeda have shown this dataset to be inaccurate in the central and coastal regions in the Java Sea. Thus, ETOPO1 dataset was also used. ETOPO1 is a 1 arc-minute global relief model of Earth's surface that integrates land topography and ocean bathymetry (*ETOPO1 Arc-Minute Global Relief Model : Procedures, Data Sources and Analysis*, n.d.).

The simulation was forced with thirteen tidal components applied at the boundaries, using TPXO data (*OSU Tidal Data Inversion*, n.d.). The tidal constituents that were used were eight primary (M2, S2, N2, K2, K1, O1, P1, Q1), two long-period (Mf, Mm) and 3 non-linear (M4, MS4, MN4) harmonic constituents (2N2 and S1). The current model has a ramp-up duration of 2 days, and an additional simulation of the model for 30 days was done. The velocity time series, depth profile and surface elevation data were obtained.

The depth average velocity profile obtained by the hydrodynamic model depicted the

water flow in the Lombok straits over a certain time. The variation of the velocity in the region the Lombok straits showed a maximum value of 2.3 m/s as shown in Figure 19. This high value of the water flow makes this site of the Indonesian waters as a suitable place for the harness of the tidal energy.

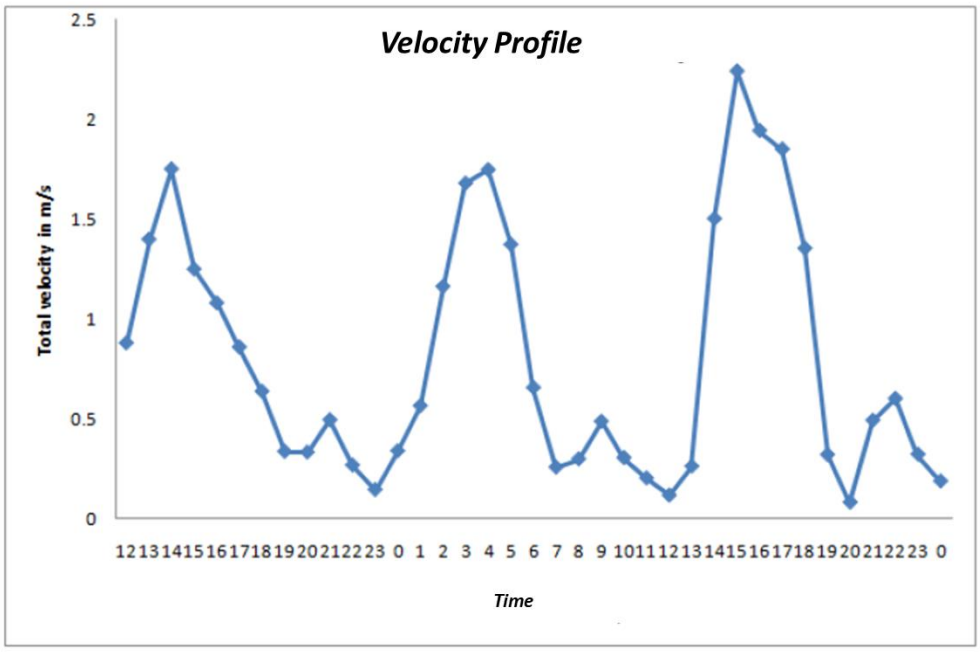

Figure 19: *Velocity Time series data*

There were atleast sixteen tidal elevation measurement stations in the model domain, that can be used for the purpose of recording data for validation. These are located in the area of ports or navigation channels. For the present validation purpose, the data from Nusa Penida Island was taken into account. The present prediction was well in line with the ADCP data as shown in Figure 20. The ocean model predicted was with a root mean square error of about 5 - 10 %.

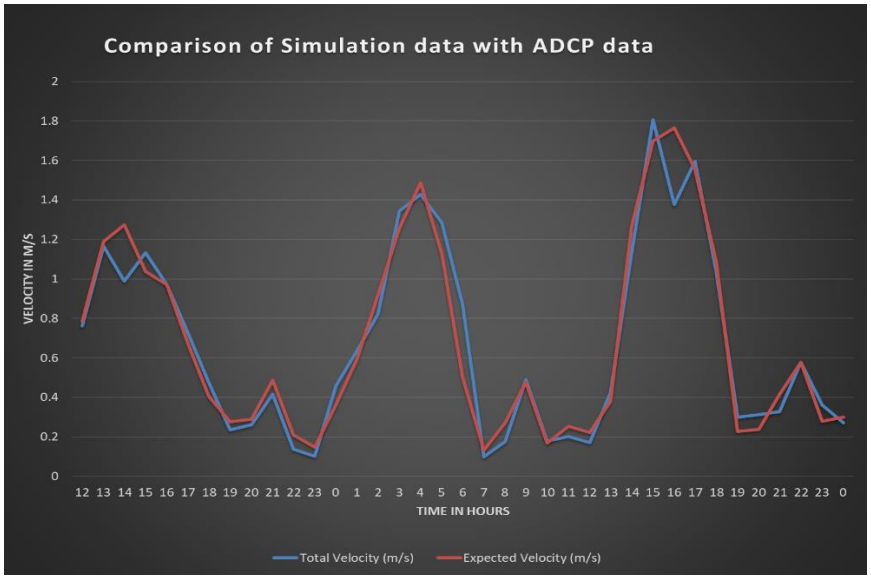

Figure 20: *Comparison of simulation results with ADCP data*

6.3 Method 3

The tidal flow of the Lombok Strait was simulated with Telemac2D. The computational domain covered a 400km x 300km area with cell size ranging from approximately 5km at the open boundaries to 400m in the zone of interest. The choice of the minimum cell size (400m) was constrained by the (low) resolution of the GEBCO bathymetric database (Kapoor, 1981). The model was forced by water elevations predicted from the TPXO9 atlas (v4a) (*OSU Tidal Data Inversion*, n.d.), which contained 8 tidal constituents: M2, S2, N2, K2, K1, O1, P1, Q1. The turbulence closure relied on the k-epsilon. The friction was simulated with a Strickler formulation. Meteorological and wave effects were disregarded.

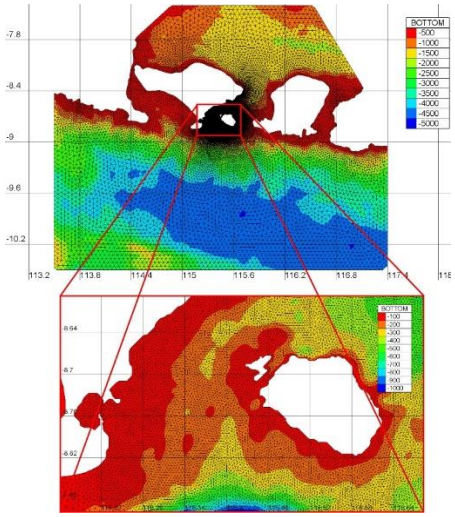

Figure 21: *Computational domain used in Telemac-2D*

The model predictions were compared to ADCP measurements acquired in the waters of Lombok during a 10-day period starting in April, 4th, in 2008. Results are illustrated in Figure 22. This figure shows that the agreement with measurements is very poor with a great underestimation of peak velocities. Different reasons can explain this misfit. The first one is the lack of accurate bathymetric dataset, especially in the vicinity of the location where the ADCP was deployed. Indeed, in the waters of Nusa Lembongan Island, depth variations of 100 m can be observed over distances of 1km. It is clear that the resolution of the GEBCO data is not sufficient to capture the complexity of the coastal morphology, especially the abrupt changes of depth, in this zone. Other reasons may explain the discrepancies between model and measurements: the vertical recirculation of the currents (that cannot be approached by a 2D model), the wake effects caused by the Nusa Lembongan Island (that may not be accurately captured by our model, partly because of the coarse mesh), the meteorological and wave effects (that have been neglected here), the limited number of tidal constituents...

The setting-up of the model did not follow the methodology required for a reliable tidal resource assessment, such as the one described in the technical specification IEC TS 62600-201. In particular, the model has not been calibrated (at the scale of the coastal region and then at the scale of the tidal Stream Energy site) with a variety of measurements (tidal gauges, bottom mounted and towed ADCP…). So, it is no surprise to obtain such a misfit. To conclude, the model limitation certainly arises from the lack of physics of the simple configuration of Telemac-2D retained here, but above all to the lack of various kinds of accurate field data required to set-up, calibrate and validate the model.

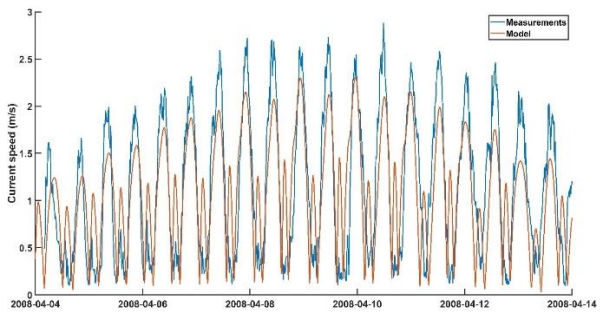

Figure 22: *Comparison between (depth-averaged) current speed predicted by the model and measured by ADCP.*

6.4 Method 4

Lombok Strait is a complex tidal channel, where tidal currents are modulated by barotropic energy fluxes from the Indian and Pacific oceans, meteorological conditions and Indonesian Throughflow (Gordon, 2005; Goward Brown et al., 2019; Ray et al., 2005). Thus, to capture the hydrokinetic energy available in the Lombok Strait that is available for harnessing through tidal turbines, the driving forces listed above should be considered (Orhan et al., 2017).

Within the framework of this study, and to serve the purpose of comparing the outcomes from different modelling systems, Delft3D modelling system has been utilized by the team from Germany, and results of the ad hoc simulations are demonstrated. Figure 23 visualizes the model domain and bathymetry.

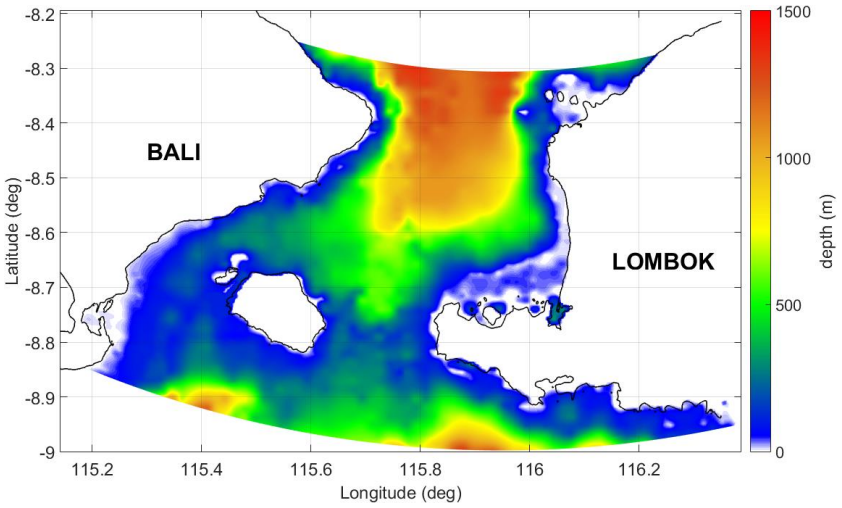

Figure 23: *Domain and bathymetry of the Delft3D FLOW model.*

FLOW module of Delft3D has been utilized to capture the tidal currents in Lombok Strait, and to save computation time, ad hoc simulations were run in 2D. A circular grid with ca. 300m horizontal resolution has been developed for orthogonality, and to capture currents in the channel with sufficient spatial resolution (*Assessment of Tidal Energy Resource*, n.d.). The model bathymetry was obtained from GEBCO gridded bathymetric database (Kapoor, 1981). Although Brown et al. (2019) argue that the ITF has a significant influence on Lombok Strait currents, which alters the current speeds in the channel up to around 40%, for the sake of simplicity and putting the emphasis on barotropic (tidal) energy flux, only tidal and meteorological driving forces have been considered in Lombok Strait Delft3D FLOW model. Tidal harmonics have been derived from the TPXO database, and the GFS database has been used to define

meteorological conditions (*Global Forecast System (GFS)*, 2020). The model accounts for turbulent kinetic energy dissipation via the k-ε turbulence closure scheme and also considers horizontal large eddies. The simulations were run for a neap-spring tidal cycle.

Results of the ad hoc simulations show that the Delft3D modelling system captures highly energetic tidal currents to the west and east of Penida Island, over a long stretch between Bali and Lombok Islands. The average current speeds calculated within this region exceed about 1.5m/s, with a standard deviation of ca. 0.8 m/s (see Figure 24). Figure 24 demonstrates the distribution of the hydrokinetic power density in Lombok Strait, which was calculated as explained in detail in the following section, and highlights the areas with a power density sufficient to be harnessed via tidal current turbines (*Potential Hydrodynamic Impacts and Performances of Commercial-Scale Turbine Arrays in the Strait of Larantuka, Indonesia* | *Tethys*, n.d.). To highlight the suitable areas for tidal energy extraction, the threshold kinetic power density has been accepted as 0.5kW/m2, which corresponds to the cut-in velocity of state-of-the-art tidal turbines.

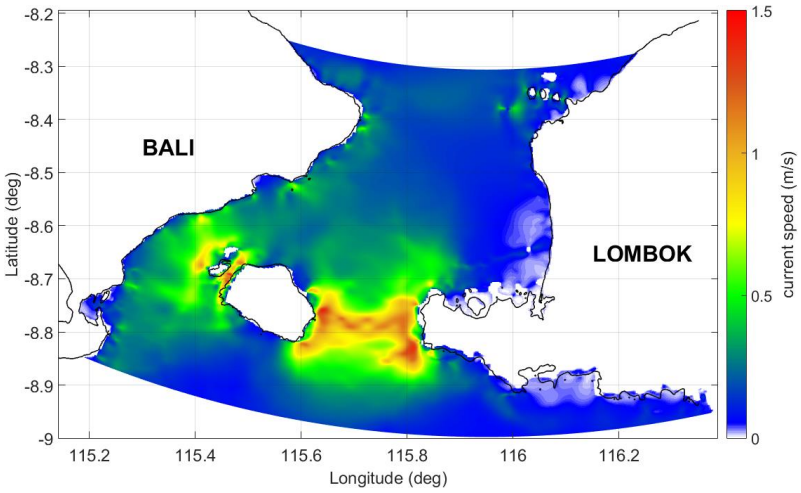

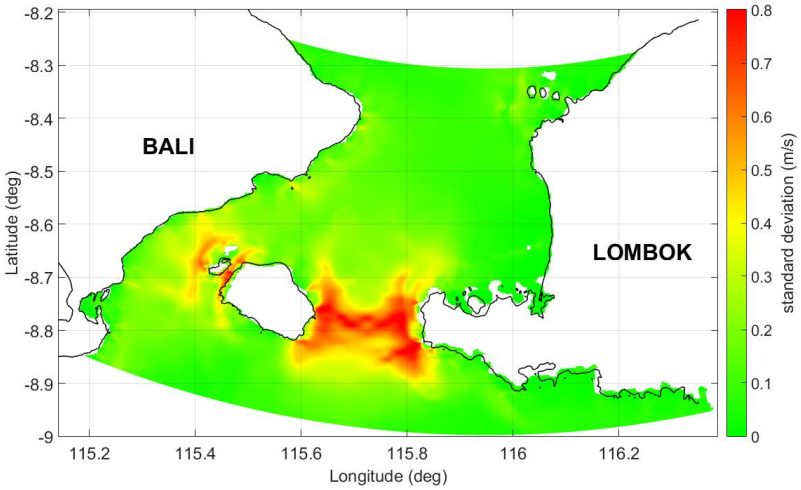

Figure 24: *Average magnitudes (top) and standard deviations (bottom) of the simulated current speeds in Lombok Strait.*

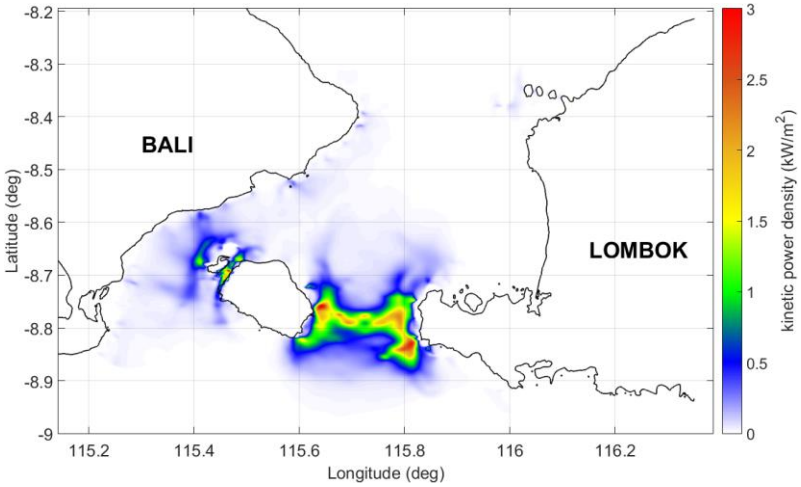

Figure 25: *Areas with hydrokinetic power density suitable for harnessing.*

As stated above for the example of the GEBCO Gridded Bathymetric Database, open-access bathymetric databases often fail to capture the seabed topography in narrow tidal channels with sufficient detail and/or precision. The bathymetric data with sufficient quality, especially for around Penida Island, was not available to the team in Germany at the time of model development. Since the ADCP data available was from near Penida Island, calibration/validation efforts have been delayed until the necessary bathymetric data is acquired. Currently, the efforts have been focused on:

- Acquiring the necessary bathymetric data from national agencies in Indonesia
- Improving grid resolution around Penida Island to reproduce the seabed topography adequately, capture the tidal currents with higher spatial resolution and simulate the potential impacts of tidal energy extraction

- Accounting for the influence of ITF through the transport conditions involved at the open sea boundaries

Nevertheless, earlier studies as well as the preliminary results acquired within the framework of this collaboration indicate that Delft3D can provide a valuable tool for the assessment of tidal current energy resources and Lombok Strait might prove a very promising domain for producing renewable electricity from tidal currents.

7. Solutions to some of the Tidal modelling & Turbine selection issues addressed in the workshop.

7.1 Effect of Seabed Roughness on Tidal Resource Prediction

Tidal predictions appear however sensitive to the value retained for the roughness parameter over rock outcrops. Increasing seabed roughness (z0) results thus in a decrease of tidal current amplitude at both measurement points with associated mean relative errors MRE_{rel} decreasing from 2.2 to - 2.8 % at location 1, and from 24.0 to 11.3 % at location 2. As predictions of current direction at location 1 are barely sensitive to bottom roughness parameterisation, a foremost calibration of z_0 over rock outcrops is determined on the basis of predicted amplitudes at this measurement point. Best comparisons are obtained for roughness parameters between 15 and 20 mm with MRE_{rel} between -0.47 and 0.08 %. More significant sensitivity to roughness of rock outcrops is however obtained at point location 2. Whereas the mean relative error of |U| is found to decrease by increasing the roughness parameter, best estimations of current direction are obtained for values of z_0 below 20 mm. As the index of agreement RE of predicted current directions at location 2 reaches a maximum value for z_0 = 30 mm, a bottom roughness parameter of 20 mm is considered as the best compromise to provide optimal predictions of tidal currents at both measurement points. Over this area, mean and maximum tidal kinetic energies are thus reduced in the same proportion, by around 30 %, between configurations with z_0 = 3.5 and 50 mm over rock outcrops. This result exhibits the great sensitivity of numerical assessment of available stream power to bottom roughness of rock outcrops in the Strait.

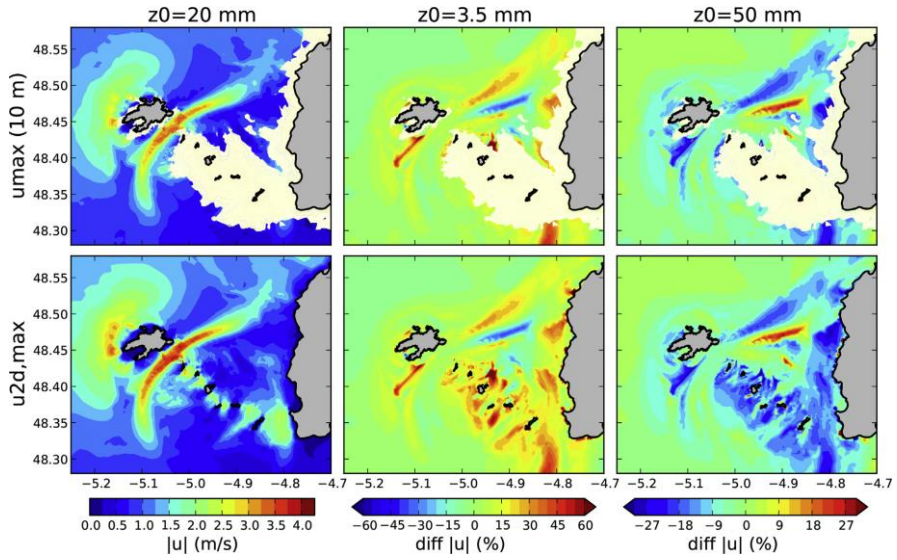

Figure 26: Maximum amplitudes of currents 10 m above the bed (umax(10 m)) and of depth-averaged currents (u2d,max) during mean spring tidal conditions for simulation with z0 = 20 mm over rock outcrops (middle and right)

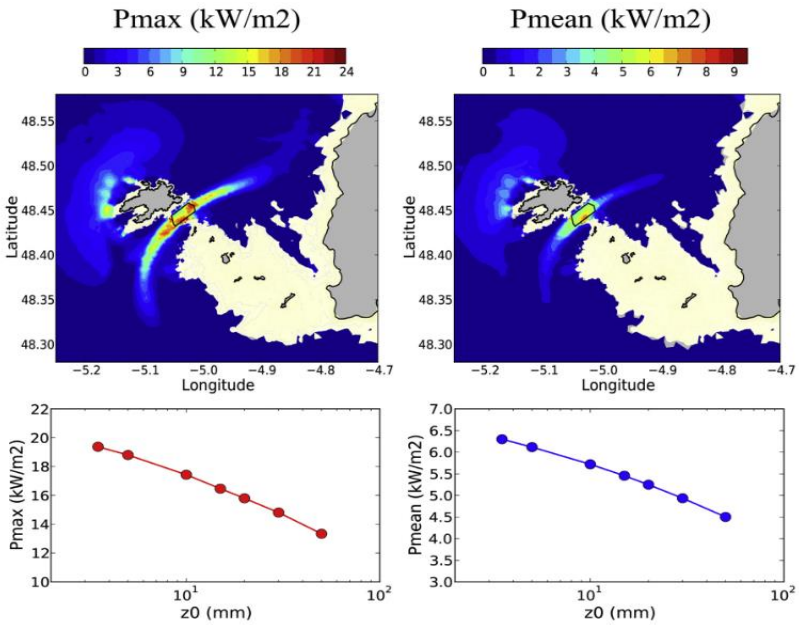

Figure 27: Maximum and mean predicted tidal stream powers 10 m above the bed during mean spring conditions for the reference configuration (z0 = 20 mm over rock outcrops).

Thus, in temperate waters, surface roughness influences the estimates of tidal kinetic energy in the area identified for stream-array implementation with a reduction of available power by 30% by rising z_0 from 3.5 to 50 mm.

7.2 Effect of Wave on Tidal Current

The effect of waves upon the tidal velocity profile was investigated for the temperate

tidal Stream Energy site. A dynamically coupled tide-wave model was applied to this domain, with characteristics similar to that of typical first generation tidal Stream Energy sites (in tidal velocities, wave climate, and water depths). A curvilinear grid (minimum grid size of 110 m by 92 m at the headland tip, maximum grid size of 1990 m by 1690 m offshore) was used to discretise a domain 50 km (east-west) by 25 km (north-south), with a parabolic headland running along the southern boundary, and depth increasing linearly from a minimum of 4 m (at the headland) to a constant depth of 40 m, 3 km off-shore.

The direct effect on the tidal Stream Energy re-source was calculated as a change in the net power available over a tidal cycle due to wave-induced modification of the tidal velocity. An M2 tidal flow (from 0.43 m/s to 0.5 m/s at the northern edge) and elevation (0.6 to 0.71m), at the west and eastern boundary are imposed as a clamped free surface open radiation condition. An average wave height of 3.79m (Hs) and period (T) of 9s was recorded at the tidal energy site. Wave direction at the analysis site varied between 78°N and 92°N (mean direction of 83°N) due to wave-tide interaction and bathymetry refraction. Therefore, we assume “east” wave conditions to be inline to the tidal flow.

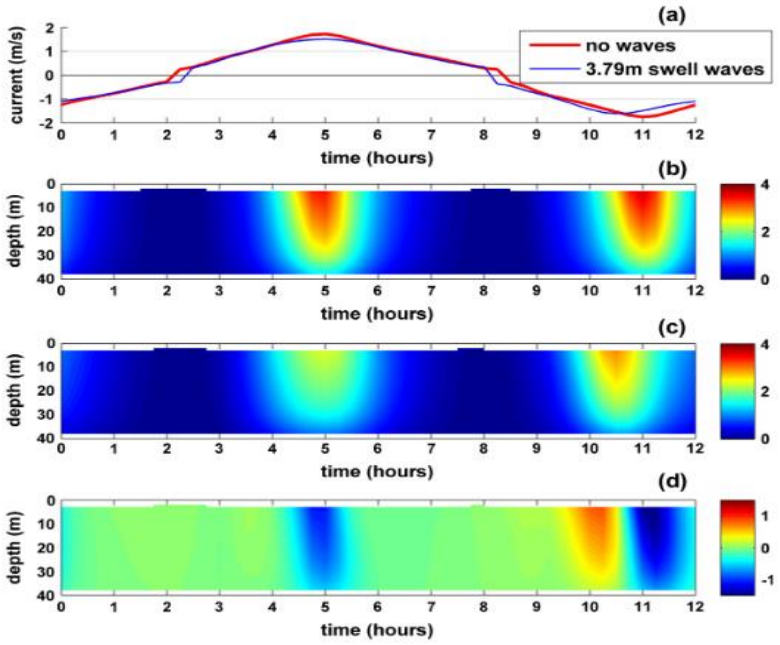

Figure 28: Average tidal current speed due to waves

Findings from the model are as follows:

- Waves reduce tidal velocities by a small amount in 40 m water depth which is

mainly attributed to waves increasing the apparent bed roughness.

- A strong linear relationship was found (R^2 of 94%) between the wave height and the net power available over a tidal cycle (both theoretical and practical tidal Stream Energy resource).
- Therefore, the wave climate, including wave direction (relative to the current), should be considered when selecting sites suitable for tidal Stream Energy arrays.

7.3 Effect of Tidal Turbine array in Flow Field

The energy of the tidal currents in the strait is assumed to be extracted by horizontal-axis tidal turbines, positioned on sequential rows, and in alternating downstream arrangements where the flow is bounded by the seabed and the free surface. The device, which can harness a strongly bi-directional flow, was assumed to have a rotor diameter of about 16 m corresponding to a swept area of about 201 m2. The minimum operational depth of the device was considered as 25 m. Rated, cut-in, and cut-out current speeds of the device were defined as 3.0 m/s, 1.0 m/s, and 4.5 m/s, respectively, and its rated power is about 1 MW. Considering the efficiencies of the various components, namely the turbine rotor, drive train, generator, and grid connection, the turbine power coefficient has been assumed as 0.41 (Orhan et al., 2017; Orhan & Mayerle, 2017; Roberts et al., 2016). The spacing between rows and lateral spacing between the devices was set to about 10 RD (rotor diameter) and 3 RD, respectively (*Assessment of Tidal Energy Resource*, n.d.; Chen et al., 2017; Orhan & Mayerle, 2017). To capture the changes occurring in the flow field in response to increasing array capacities, the proposed layout consists of 2,4,6 and 8 rows of turbines comprising of a total of 6,15,24 and 35 devices.

Findings from the model are as follows:

- Turbine arrays could cause significant changes in the flow field of a location.
- Increased numbers of rows and turbines deployed resulted in a deficit of about 0.5–0.6 m/s. This corresponds to decreases in current speeds of about 25 – 30 % average.
- Stronger current velocities were observed on the sides, closer to the banks due to the geometry of the strait and the proximity of turbines to the banks and near-

shore shallow waters.

7.4 Normalisation of Tidal Turbines

Tidal-Stream Energy resource can be predicted deterministically, provided tidal harmonics and turbine device characteristics are known. Many turbine designs exist, all having different characteristics (e.g., rated speed), which creates uncertainty in resource assessment or renewable energy system-design decision-making. A standardised normalised tidal-stream power-density curve was parameterised with data from 14 operational horizontal-axis turbines as shown in Figure 29 (e.g., mean cut-in speed was ~30% of rated speed). Horizontal-axis tidal-stream turbine power density curves were normalised and standardised, which can be applied to idealised tidal current time-series with increasing complexity in tidal harmonics, and then applied to global tidal harmonic data.

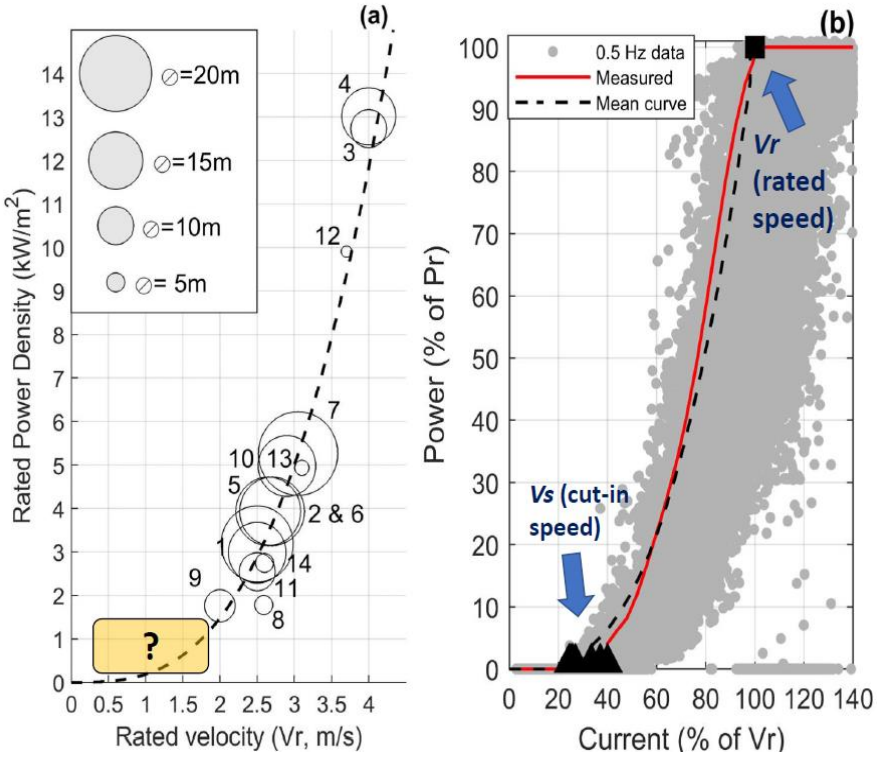

Figure 29: *Tidal-stream turbine characteristics from 14 commercially developed devices*

Findings from the study are as follows:

(1) Tidal-turbine cut-in speed (Vs) was found to be ~30% of rated turbine speed (Vr) on average.

(2) For a deployment concerned with near-maximum yield aspirations, rated tidal-stream turbine speed (Vr) at a given site will be ~87% to 97% of site maximum flow respectively

(3) Deployments concerned with firm, constant power and small amounts of storage, may aim to deploy tidal-stream turbines with much lower rated speeds (~56% of site maximum flow), with spatial variability due to resource (maximum current speed) and the tidal form (F value) – due to the nature of the tide at a given site.

(4) Average values of normalised data from fourteen horizontal axis tidal-stream turbines, alongside estimation of optimal cut-in and rated speed, allowed a standardised power curve and device behaviour to be implemented in resource and environmental impact assessment, without bias to one specific design to allow tidal energy resource mapping for future technologies.

8. Common Representation of Results

8.1 Hydrokinetic Power of Tidal Turbine

To analyze the hydrokinetic power of tidal currents is important to realize that this power has a direct relationship with the velocities involved. Specifically, the tidal current power per m2 is defined as

$$P = \frac{1}{2}\rho V^3$$

where,
P is the hydrokinetic power (W/m2)
v is the velocity of the current (m/s)
ρ is the water density (kg/m3)

8.2 Power Density

The average power density (APD) available across the surface area considered should be calculated from the time series of the predicted velocity distribution f(Ui). The APD shall be calculated with the equation below where N_B is the number of bins and the index i refers to the bin number:

$$APD = \frac{1}{2} \cdot \rho \cdot \sum_{i=1}^{N_B} \left(U_i^3 \cdot f(U_i) \right) = \frac{1}{2} \rho \cdot V_{rmc}^3 \quad (\mathrm{kW/m^2})$$

Ui is the central value of the i^{th} bin, and V_{rmc} is the root mean cubed velocity, to be calculated with the equation below:

$$V_{rmc} = \sqrt[3]{\sum_{i=1}^{N_B} \left(U_i^3 \cdot f(U_i) \right)} \quad (\mathrm{m/s})$$

8.3 Annual Energy Production

For each tidal turbine, the annual energy production (AEP) can be obtained by combining the P with the rotor area , available hours per year and turbine efficiency:

$$AEP = \mathrm{P} \times C_p \times \mathrm{A} \times 8760 \ \left(\frac{\mathrm{kWh}}{\mathrm{year}} \right)$$

9. Conclusion

Lack of tidal energy resource information becomes a barrier to tidal energy adoption into a nation's energy mix. There is not much awareness to the stakeholders on various tools and techniques available to identify the tidal energy resource. Knowledge of chosen hydrodynamic model's accuracy is lacking with certainties concerning the available resources by practical users. Thus, the present report highlighted the various modelling strategies along with few case studies to highlight the accuracies of each models. In temperate waters, seabed surface roughness influences the estimates of tidal kinetic energy in the area identified for stream-array implementation with a reduction of available power by 30% by rising z0 from 3.5 to 50 mm. Reduction in tidal velocity due to attribution of waves increasing the apparent bed roughness was also found. Effect of tidal turbine arrays also causes significant changes in the flow field of a location. Standardized power curve and device behavior can be implemented in resource and environmental impact assessment without bias to one specific design to allow tidal energy resource mapping for future technologies. With such clear resource understanding sizing of systems would be more accurate through site-tidal turbine

systems matching. Risk in project planning and execution of tidal array farms can also be reduced.

10. References

A Hierarchy of Turbulence Closure Models for Planetary Boundary Layers in: Journal of the Atmospheric Sciences Volume 31 Issue 7 (1974). (n.d.). Retrieved July 26, 2023, from https://journals.ametsoc.org/view/journals/atsc/31/7/1520-0469_1974_031_1791_ahotcm_2_0_co_2.xml

ADA318516.pdf. (n.d.). Retrieved July 26, 2023, from https://apps.dtic.mil/sti/pdfs/ADA318516.pdf

ADCIRC: An Advanced Three-Dimensional Circulation Model for Shelves, Coasts, and Estuaries. Report 1. Theory and Methodology of ADCIRC-2DDI and ADCIRC-3DL. (n.d.).

Adcock, T. A. A., Draper, S., Houlsby, G. T., Borthwick, A. G. L., & Serhadlıoğlu, S. (2013). The available power from tidal stream turbines in the Pentland Firth. Proceedings of the Royal Society A: Mathematical, Physical and Engineering Sciences, 469(2157), 20130072. https://doi.org/10.1098/rspa.2013.0072

An s coordinate density evolving model of the northwest European continental shelf: 1. Model description and density structure—Holt—2001—Journal of Geophysical Research: Oceans—Wiley Online Library. (n.d.). Retrieved July 26, 2023, from https://agupubs.onlinelibrary.wiley.com/doi/10.1029/2000JC000304

Assessment of Tidal Energy Resource: EMEC: European Marine Energy Centre. (n.d.). Retrieved October 12, 2022, from https://www.emec.org.uk/assessment-of-tidal-energy-resource/

Assessment of tidal power opportunities in Indonesian waters—ORA - Oxford University Research Archive. (n.d.). Retrieved July 26, 2023, from https://ora.ox.ac.uk/objects/uuid:a73a007d-5b0f-48cb-8a26-3aa1ba3da262

Bishop-Taylor, R., Nanson, R., Sagar, S., & Lymburner, L. (2021). Mapping Australia's dynamic coastline at mean sea level using three decades of Landsat imagery. Remote Sensing of Environment, 267, 112734. https://doi.org/10.1016/j.rse.2021.112734

Bryden, I., & Couch, S. (2006). ME1 - Marine energy extraction: Tidal resource analysis. Renewable Energy, 31, 133–139. https://doi.org/10.1016/j.renene.2005.08.012

Casulli, V., & Walters, R. A. (2000). An unstructured grid, three-dimensional model based on the shallow water equations. International Journal for Numerical Methods in Fluids, 32(3), 331–348. https://doi.org/10.1002/(SICI)1097-0363(20000215)32:3<331::AID-FLD941>3.0.CO;2-C

Chen, Y., Lin, B., Lin, J., & Wang, S. (2017). Experimental study of wake structure behind a horizontal axis tidal stream turbine. Applied Energy, 196, 82–96. https://doi.org/10.1016/j.apenergy.2017.03.126

Climate Data Online (CDO)—The National Climatic Data Center's (NCDC) Climate Data Online (CDO) provides free access to NCDC's archive of historical weather and climate data in addition to station history information. | National Climatic Data Center (NCDC). (n.d.). Retrieved July 26, 2023, from https://www.ncei.noaa.gov/cdo-web/

Coles, D. S., Blunden, L. S., & Bahaj, A. S. (2017). Assessment of the energy extraction potential at tidal sites around the Channel Islands. Energy, 124, 171–

186. https://doi.org/10.1016/j.energy.2017.02.023

Competition effects between nearby tidal turbine arrays—Optimal design for the Alderney Race. (n.d.). Retrieved July 26, 2023, from https://bibbase.org/network/publication/goes-piggott-kramer-avdis-angeloudis-cotter-competitioneffectsbetweennearbytidalturbinearraysoptimaldesignforthealderneyrace-2018

Design and development of DELFT3D and application to coastal morphodynamics. (n.d.). Retrieved July 26, 2023, from https://www.infona.pl/resource/bwmeta1.element.elsevier-1ca19bb6-25b9-3bf5-bfe9-e96a7027c553

DHI. (n.d.). Retrieved July 26, 2023, from https://www.dhigroup.com/download/mike-by-dhi-tools/coastandseatools/global-tide-model

Draper, S., Adcock, T. A. A., Borthwick, A. G. L., & Houlsby, G. T. (2014). Estimate of the tidal stream power resource of the Pentland Firth. Renewable Energy, 63(C), 650–657.

Egbert, G. D., & Erofeeva, S. Y. (2002). Efficient Inverse Modeling of Barotropic Ocean Tides. Journal of Atmospheric and Oceanic Technology, 19, 183–204. https://doi.org/10.1175/1520-0426(2002)019<0183:EIMOBO>2.0.CO;2

Egbert, G., Erofeeva, S., & Ray, R. (2010). Assimilation of altimetry data for nonlinear shallow-water tides: Quarter-diurnal tides of the Northwest European Shelf. Continental Shelf Research, 30, 668–679. https://doi.org/10.1016/j.csr.2009.10.011

ETOPO Global Relief Model | National Centers for Environmental Information (NCEI).

(n.d.). Retrieved July 26, 2023, from https://www.ncei.noaa.gov/products/etopo-global-relief-model

ETOPO1 arc-minute global relief model: Procedures, data sources and analysis. (n.d.). Retrieved October 12, 2022, from https://repository.library.noaa.gov/view/noaa/1163

Firdaus, A., Houlsby, G., & Adcock, T. (2019, September 9). Resource estimates in Lombok Straits, Indonesia.

FVCOM (the unstructured grid Finite Volume Community Ocean Model) | Model Item | OpenGMS. (n.d.). Retrieved August 3, 2023, from https://geomodeling.njnu.edu.cn/modelItem/5738ef7c-a5ac-46b5-a347-3c823f71b3a7

Galperin, B., Kantha, L. H., Hassid, S., & Rosati, A. (1988). A Quasi-equilibrium Turbulent Energy Model for Geophysical Flows. Journal of the Atmospheric Sciences, 45(1), 55–62. https://doi.org/10.1175/1520-0469(1988)045<0055:AQETEM>2.0.CO;2

Global Forecast System (GFS). (2020, August 12). National Centers for Environmental Information (NCEI). https://www.ncei.noaa.gov/products/weather-climate-models/global-forecast

Gordon, A. (2005). Oceanography of the Indonesian Seas and Their Throughflow. Oceanography, 18, 14–27. https://doi.org/10.5670/oceanog.2005.01

Goss, Z., Warder, S., Angeloudis, A., Kramer, S. C., Avdis, A., & Piggott, M. D. (n.d.). Tidal modelling with Thetis: Preliminary English Channel benchmarking.

Goward Brown, A. J., Lewis, M., Barton, B. I., Jeans, G., & Spall, S. A. (2019). Investigation of the Modulation of the Tidal Stream Resource by Ocean

Currents through a Complex Tidal Channel. Journal of Marine Science and Engineering, 7(10), 341. https://doi.org/10.3390/jmse7100341

GSHHG - A Global Self-consistent, Hierarchical, High-resolution Geography Database. (n.d.). Retrieved July 24, 2023, from https://www.soest.hawaii.edu/pwessel/gshhg/

Hersbach, H., Bell, B., Berrisford, P., Hirahara, S., Horányi, A., Muñoz-Sabater, J., Nicolas, J., Peubey, C., Radu, R., Schepers, D., Simmons, A., Soci, C., Abdalla, S., Abellan, X., Balsamo, G., Bechtold, P., Biavati, G., Bidlot, J., Bonavita, M., … Thépaut, J.-N. (2020). The ERA5 global reanalysis. Quarterly Journal of the Royal Meteorological Society, 146(730), 1999–2049. https://doi.org/10.1002/qj.3803

Hervouet, J.-M. (2007). Hydrodynamics of Free Surface Flows: Modelling With the Finite Element Method. Hydrodynamics of Free Surface Flows: Modelling with the Finite Element Method. https://doi.org/10.1002/9780470319628

Hodges, B. (2000). Numerical Techniques in CWR-ELCOM (code release v.1).

Houlsby, G., Draper, S., & Oldfield, M. (2008). Application of Linear Momentum Actuator Disc Theory to Open Channel Flow.

Houlsby, G., & Vogel, C. (2016). The power available to tidal turbines in an open channel flow. Proceedings of the Institution of Civil Engineers - Energy, 170, 1–10. https://doi.org/10.1680/jener.15.00035

Identification of Characteristics Influencing Wave Height and Current Velocity in MIKE Model for Simulation of Wind-induced Ocean Currents and Waves in Southeast of Caspian Sea. (n.d.). Retrieved July 26, 2023, from https://www.ijee.net/article_119991.html

Kapoor, D. C. (1981). General bathymetric chart of the oceans (GEBCO). Marine Geodesy, 5(1), 73–80. https://doi.org/10.1080/15210608109379408

Kurniawan, A., Barli, P. P. A., Pratama, M., & Fitriadhy, A. (2021). Potential Study of Tidal Stream Turbine Farm at Toyapakeh Strait, Bali. ILMU KELAUTAN: Indonesian Journal of Marine Sciences, 26, 155–162. https://doi.org/10.14710/ik.ijms.26.3.155-162

Le Provost, C., Genco, M. L., Lyard, F., Vincent, P., & Canceil, P. (1994). Spectroscopy of the world ocean tides from a finite element hydrodynamic model. Journal of Geophysical Research, 99(C12), 24777. https://doi.org/10.1029/94JC01381

Luettich, J., Richard, & Westerink, J. (2004). Formulation and Numerical Implementation of the 2D/3D ADCIRC Finite Element Model Version 44.XX.

Lyard, F. H., Allain, D. J., Cancet, M., Carrère, L., & Picot, N. (2021). FES2014 global ocean tide atlas: Design and performance. Ocean Science, 17(3), 615–649. https://doi.org/10.5194/os-17-615-2021

MNT Bathymétrique de façade Atlantique (Projet Homonim) NM. (n.d.). Catalogue Shom. Retrieved July 26, 2023, from https://services.data.shom.fr:/geonetwork/srv/api/records/MNT_ATL100m_HOMONIM_WGS84_NM_ZNEG.xml

National Ocean Service (NOS) Hydrographic Survey | National Centers for Environmental Information (NCEI). (n.d.). Retrieved July 26, 2023, from https://www.ncei.noaa.gov/products/nos-hydrographic-survey

Neill, S. P. (2008). The role of Coriolis in sandbank formation due to a headland/island system. Estuarine, Coastal and Shelf Science, 79(3), 419–428.

https://doi.org/10.1016/j.ecss.2008.04.015

Neill, S. P., Angeloudis, A., Robins, P. E., Walkington, I., Ward, S. L., Masters, I., Lewis, M. J., Piano, M., Avdis, A., Piggott, M. D., Aggidis, G., Evans, P., Adcock, T. A. A., Židonis, A., Ahmadian, R., & Falconer, R. (2018). Tidal range energy resource and optimization – Past perspectives and future challenges. Renewable Energy, 127, 763–778. https://doi.org/10.1016/j.renene.2018.05.007

NRL 7320: NRL DBDB2. (n.d.). Retrieved July 26, 2023, from https://www7320.nrlssc.navy.mil/DBDB2_WWW/

Orhan, K., & Mayerle, R. (2017). Assessment of the tidal stream power potential and impacts of tidal current turbines in the Strait of Larantuka, Indonesia. Energy Procedia, 125, 230–239. https://doi.org/10.1016/j.egypro.2017.08.199

Orhan, K., Mayerle, R., Narayanan, R., & Pandoe, W. (2017). INVESTIGATION OF THE ENERGY POTENTIAL FROM TIDAL STREAM CURRENTS IN INDONESIA. Coastal Engineering Proceedings, 35, 10. https://doi.org/10.9753/icce.v35.management.10

OSU Tidal Data Inversion. (n.d.). Retrieved July 26, 2023, from http://g.hyyb.org/archive/Tide/TPXO/TPXO_WEB/atlas.html

Piccioni, G., Dettmering, D., Bosch, W., & Seitz, F. (2019). TICON: TIdal CONstants based on GESLA sea-level records from globally located tide gauges. Geoscience Data Journal, 6(2), 97–104. https://doi.org/10.1002/gdj3.72

Potential Hydrodynamic Impacts and Performances of Commercial-Scale Turbine Arrays in the Strait of Larantuka, Indonesia | Tethys. (n.d.). Retrieved August 2, 2023, from https://tethys.pnnl.gov/publications/potential-hydrodynamic-

impacts-performances-commercial-scale-turbine-arrays-strait

Ray, R., Egbert, G., & Erofeeva, S. (2005). A Brief Overview of Tides in the Indonesian Seas. Oceanography, 18(4), 74–79. https://doi.org/10.5670/oceanog.2005.07

Roberts, A., Thomas, B., Sewell, P., Khan, Z., Balmain, S., & Gillman, J. (2016). Current tidal power technologies and their suitability for applications in coastal and marine areas. Journal of Ocean Engineering and Marine Energy, 2(2), 227–245. https://doi.org/10.1007/s40722-016-0044-8

Roe, P. L. (1981). Approximate Riemann solvers, parameter vectors, and difference schemes. Journal of Computational Physics, 43(2), 357–372. https://doi.org/10.1016/0021-9991(81)90128-5

Schmitt, T., Schaap, D., Spoelstra, G., Benoit, L., & Cyrille, P. (2019, June 26). EMODnet Bathymetry a compilation of bathymetric data in the European waters. https://doi.org/10.1109/OCEANSE.2019.8867250

Shchepetkin, A. F., & McWilliams, J. C. (2005). The regional oceanic modeling system (ROMS): A split-explicit, free-surface, topography-following-coordinate oceanic model. Ocean Modelling, 9(4), 347–404. https://doi.org/10.1016/j.ocemod.2004.08.002

Sheng, Y. P., & Villaret, C. (1989). Modeling the effect of suspended sediment stratification on bottom exchange processes. Journal of Geophysical Research, 94, 14,429-14,444. https://doi.org/10.1029/JC094iC10p14429

Tidal power generation – A review of hydrodynamic modelling—Thomas AA Adcock, Scott Draper, Takafumi Nishino, 2015. (n.d.). Retrieved July 26, 2023, from https://journals.sagepub.com/doi/abs/10.1177/0957650915570349

Vennell, R., Funke, S. W., Draper, S., Stevens, C., & Divett, T. (2015). Designing large

arrays of tidal turbines: A synthesis and review. Renewable and Sustainable Energy Reviews, 41(C), 454–472.

Walters, R. (2005). Coastal ocean models: Two useful finite element methods. Continental Shelf Research, 25, 775–793. https://doi.org/10.1016/j.csr.2004.09.020

WHELAN, J., GRAHAM, J., & Peiro, J. (2009). A free-surface and blockage correction for tidal turbines. Journal of Fluid Mechanics, 624, 281–291. https://doi.org/10.1017/S0022112009005916

Woodruff, S. D., Slutz, R. J., Jenne, R. L., & Steurer, P. M. (1987). A Comprehensive Ocean-Atmosphere Data Set. Bulletin of the American Meteorological Society, 68(10), 1239–1250.

Yadav, S. (n.d.). Riemann Solvers and Numerical Methods for Fluid Dynamics Third Edition. Retrieved July 24, 2023, from https://www.academia.edu/8844903/Riemann_Solvers_and_Numerical_Methods_for_Fluid_Dynamics_Third_Edition

Yesson, C., Clark, M., Taylor, M., & Rogers, A. (2011). The global distribution of seamounts based on 30 arc seconds bathymetry data. Deep-Sea Research Part I-Oceanographic Research Papers - DEEP-SEA RES PT I-OCEANOG RES, 58, 442–453. https://doi.org/10.1016/j.dsr.2011.02.004

Yousef, M., Venugopal, V., & Johanning, L. (n.d.). Tidal energy resource assessment with TELEMAC-2D of the Churchill Barriers, Scotland.

Zhang, Y., & Baptista, A. (2004). Benchmarking a new open-source 3D circulation model (ELCIRC). Developments in Water Science, 55. https://doi.org/10.1016/S0167-5648(04)80185-0

Zhang, Y. J., Ye, F., Stanev, E. V., & Grashorn, S. (2016). Seamless cross-scale modeling with SCHISM. Ocean Modelling, 102, 64–81. https://doi.org/10.1016/j.ocemod.2016.05.002

11. Annex A – Model Input Databases

11.1 Coastline Databases

Some of the common Coastline Databases are as follows:

Global Self-consistent, Hierarchical, High-resolution Geography Database (GSHHG) is a high-resolution geography data set, amalgamated from two databases: World Vector Shorelines (WVS) and CIA World Data Bank II (WDBII) (*GSHHG - A Global Self-Consistent, Hierarchical, High-Resolution Geography Database*, n.d.). The former is the basis for shorelines while the latter is the basis for lakes, although there are instances where differences in coastline representations necessitated adding WDBII islands to GSHHG. The WDBII source also provides political borders and rivers. GSHHG data have undergone extensive processing and should be free of internal inconsistencies such as erratic points and crossing segments. The shorelines are constructed entirely from hierarchically arranged closed polygons. GSHHG combines the older GSHHS shoreline database with WDBII rivers and borders, available in either ESRI shapefile format or in a native binary format. Geography data are in five resolutions: crude(c), low(l), intermediate(i), high(h), and full(f). Shorelines are organized into four levels: boundary between land and ocean (L1), boundary between lake and land (L2), boundary between island-in-lake and lake (L3), and boundary between pond-in-island and island (L4). Datasets are in WGS84 geographic (simple latitudes and longitudes; decimal degrees).

The **EEA coastline dataset** has been created for detailed analysis (e.g.:1/100000) for geographical Europe . The coastline is a hybrid product obtained from satellite imagery from two projects: EUHYDRO (Pan-European hydrographic and drainage database) and GSHHG (A Global Self-consistent, Hierarchical, High-resolution Geography Database), as well as some manual amendments to meet requirements from EU Nature Directives, Water Framework Directive and Marine Strategy Framework

Directive. In 2015, several corrections were made in the Kalogeroi Islands and two other Greek little islets, as well as in the peninsula of Porkkala. In 2017 revision, two big lagoons have been removed from Baltic region, because, according to HELCOM, are freshwater lagoons.

Digital Earth Australia Coastlines is a continental dataset that includes annual shorelines and rates of coastal change along the entire Australian coastline from 1988 to the present (Bishop-Taylor et al., 2021). The product combines satellite data from Geoscience Australia's Digital Earth Australia program with tidal modelling to map the most representative location of the shoreline at mean sea level tide for each year. The product enables trends of coastal retreat and growth to be examined annually at both a local and continental scale, and for patterns of coastal change to be mapped historically and updated regularly as data continues to be acquired. This allows current rates of coastal change to be compared with that observed in previous years or decades.

11.2 Bathymetry Databases

Some of the common Bathymetry Databases are as follows:

The Generic Bathymetry Charts of the Ocean (GEBCO) data set is the gridded bathymetry obtained from a digital bathymetric model of the world ocean floor which has been merged with the land topography (Kapoor, 1981). The GEBCO 2022 Grid is a global terrain model for ocean and land, providing elevation data, in meters, on a 15 arc-second interval grid of 43200 rows x 86400 columns, giving 3,732,480,000 data points. The data values are pixel-centre registered i.e., they refer to elevations, in meters, at the centre of grid cells. It is a continuous, global terrain model for ocean and land with a spatial resolution of 15 arc seconds. It uses as a ‘base’ version 2.4 of the SRTM15+ data set between latitudes of 50° South and 60° North. This data set is a fusion of land topography with measured and estimated seafloor topography.

Originally designed for military use, the multibeam echosounder has proved very useful for nautical charting, oceanographic research and modelling, habitat classification, maritime commerce, and recreational applications. The Multibeam Bathymetry Database at NCEI collects and archives multibeam data from the earliest commercial installations (circa 1980) through today's modern high-resolution collections (*National Ocean Service (NOS) Hydrographic Survey* | *National Centers*

for Environmental Information (NCEI), n.d.). Data are acquired from a variety of primarily government and academic sources (see individual cruise metadata records for source information) and consist of the raw (as collected) sonar data files. Datasets may also include processed or edited versions of the sonar data, ancillary data, derived products, and/or metadata for the data collection.

EMODnet Bathymetry aims to provide a single access point to bathymetric data (survey data sets and composite DTMs) and derived bathymetric data products such as best-estimate European digital coastlines, inventory of official coastlines and baselines, a series of high-resolution DTMs for selected areas, and the EMODnet Bathymetry World Base Layer OGC web service (Schmitt et al., 2019). Its flagship data product is the harmonised Digital Terrain Model (DTM) for all European sea regions with a common grid resolution which is generated and regularly updated on the basis of an increasing collection of bathymetric data sets, gathered from organisations from government, research institutes, and industry. This DTM is updated every 2 years and made available in the EMODnet Map viewer, by OGC web services, and by downloading in multiple formats for use in GIS systems and as base layer for numerical hydraulic models.

NIWA provides free New Zealand Region bathymetric datasets and images (Yesson et al., 2011). This dataset provides the most up-to-date bathymetry of one of the largest areas of deep-water seabed under national jurisdiction. The 250m resolution gridded bathymetric data set encompasses New Zealand's Exclusive Economic Zone and is available in multiple high-resolution file formats to suit a range of imagery and mapping needs.

The NRL DBDB2 is based on the Naval Oceanographic Office (NAVO) global 5-min DBDBV/DBDB5 bathymetry and includes all the DBDBV high resolution data (*NRL 7320: NRL DBDB2*, n.d.). Other high resolution bathymetry data sets such as IBCAO (Artic), DAMEE (Atlantic), MMS GOM01 (GOM), NAVO NGLI (NGOM), Choi's (JES/YES) and GA ABTG (Australia), are also incorporated. The Smith & Sandwell (1997) global seafloor topography from satellite altimetry and ship depth soundings was used for the deep water. The finest GMT (The Generic Mapping Tools) vector coastline data are applied to generate the land-sea mask. The GMT coastline data are a processed mix of the CIA's global coastline and the WVS (World Vector Shoreline) global coastline. The Naval Research Laboratory Digital Bathymetry Data Base 2-

minute resolution (NRL DBDB2) is a global topography data set on a 2-min by 2-min uniform grid developed for the ocean model.

The ETOPO Global Relief Model integrates topography, bathymetry, and shoreline data from regional and global datasets to enable comprehensive, high resolution renderings of geophysical characteristics of the earth's surface (*ETOPO Global Relief Model | National Centers for Environmental Information (NCEI)*, n.d.). The model is designed to support tsunami forecasting, modelling, and warning, as well as ocean circulation modelling and Earth visualization. The current version, ETOPO 2022, is available in Ice Surface and Bedrock versions that portray either the top layer of the ice sheets covering Greenland and Antarctica, or the bedrock.

11.3 Tidal Forcing Databases

Some of the common Tidal Forcing Databases are as follows:

Oregon State University (OSU) provides one global tidal solution (called TPXO) and several regional and local tidal solutions (G. D. Egbert & Erofeeva, 2002). For example, to model French or UK coasts, the Atlantic Ocean (AO) and the European Shelf (ES) that covers the North-East Atlantic Ocean, models exist on a structured grid, with 11 harmonic constituents (M2, S2, N2, K2, K1, O1, P1, Q1, M4, MS4 and MN4) or 13 constituents for the TPXO global solution (same as ES or AO + Mf and Mm). The solutions give amplitudes and phases for the tidal elevation and transport from which the two horizontal components of the current can be deduced (by dividing transport by water depth). The resolutions of the different models are, for example, ¼ degree for the TPXO global solution, 1/12 degree for the regional Atlantic Ocean solution and 1/30 degree for the local European Shelf solution.

FES2014 is the last version of the FES (Finite Element Solution) tide model developed in 2014-2016 (Lyard et al., 2021). It is an improved version of the FES2012 model. This new FES2014 model has been developed, implemented and validated by the LEGOS, NOVELTIS and CLS, within a CNES funded project. FES2014 takes advantage of longer altimeter time series and better altimeter standards, improved modeling and data assimilation techniques, a more accurate ocean bathymetry and a refined mesh in most of shallow water regions. Special efforts have been dedicated to address the major non-linear tides issue and to the determination of accurate tidal currents. A new global finite element grid (~2.9 million nodes, 50% more than

FES2012) is used and model physic has been improved, leading to a nearly twice more accurate 'free' solution (independent of in situ and remote-sensing data) than the previous FES2012 version. Then the accuracy of this 'free' solution was improved by assimilating long-term altimetry data (Topex/ Poseidon, Jason-1, Jason-2, TPN-J1N, and ERS-1, ERS-2, ENVISAT) and tidal gauges through an improved representer assimilation method. The tide elevations, the tide currents and the tide loading grids are available for download. 34 tidal constituents are distributed on 1/16° grids (amplitude and phase) for each tidal product: 2N2 ,EPS2 ,J1 ,K1 ,K2 ,L2 ,La2 ,M2 ,M3 ,M4 ,M6 ,M8 ,Mf ,MKS2,Mm,MN4,MS4,MSf,MSqm,Mtm,Mu2,N2,N4,Nu2,O1,P1,Q1,R2,S1,S2,S4,Sa, Ssa,T2.

MIKE 21 Global Tide model - data for tidal prediction of water levels. An improved version of the Global Tide Model is available in 0.125º x 0.125º resolution (*DHI*, n.d.). The model is updated with additional 4 years of radar satellite measurement and 2 additional constituents has been added providing better predictions of water levels in shallow water. The updated model includes the following 10 constituents: Semidiurnal: M2, S2, K2, N2 - Diurnal: S1, K1, O1, P1, Q1 - Shallow water: M4. The Global Tide Model is developed by DTU Space as an update of the AG95 ocean tide.

The Tidal CONstants (TICON) data set contains information on harmonic constants for 40 tidal constituents, derived from the GESLA tide gauge records distributed on a quasi-global scale (Piccioni et al., 2019). The tidal estimations were derived through a least squares-based harmonic analysis on the single time series after a screening for outliers and minimal observation period. TICON is a useful and easy-to-handle data set for global ocean tide model validation and has proven to be vital in understanding ocean tides. A first version of TICON based on the GESLA-2 dataset has been published in 2019. The TICON database has been recently updated based on the GESLA-3 product. This has resulted in the increase in the number of tide gauges to 3679 in the new TICON-3 database compared to the previous version with only 1145 tide gauges. TICON-3 only utilizes GESLA-3 records of at least 1-year in length and provides estimations for the amplitude and phase of 40 tidal constituents at all of these tide gauges.

11.4 Wind & Climate Database

Some of the common Wind and Climate Databases are as follows:

ERA5 provides hourly estimates of a large number of atmospheric, land and oceanic climate variables (Hersbach et al., 2020). The data cover the Earth on a 30km grid and resolve the atmosphere using 137 levels from the surface up to a height of 80km. ERA5 includes information about uncertainties for all variables at reduced spatial and temporal resolutions. Quality-assured monthly updates of ERA5 (1959 to present) are published within 3 months of real time. Preliminary daily updates of the dataset are available to users within 5 days of real time. ERA5 combines vast amounts of historical observations into global estimates using advanced modelling and data assimilation systems.

Climate Data Online (CDO) provides free access to NCDC's archive of global historical weather and climate data in addition to station history information (*Climate Data Online (CDO) - The National Climatic Data Center's (NCDC) Climate Data Online (CDO) Provides Free Access to NCDC's Archive of Historical Weather and Climate Data in Addition to Station History Information.* | *National Climatic Data Center (NCDC)*, n.d.). These data include quality controlled daily, monthly, seasonal, and yearly measurements of temperature, precipitation, wind, and degree days as well as radar data and 30-year Climate Normals. Customers can also order most of these data as certified hard copies for legal use.

The International Comprehensive Ocean-Atmosphere Data Set (ICOADS) is a global ocean marine meteorological and surface ocean dataset (Woodruff et al., 1987). It is formed by merging many national and international data sources that contain measurements and visual observations from ships (merchant, navy, research), moored and drifting buoys, coastal stations, and other marine and near-surface ocean platforms. Each marine report contains individual observations of meteorological and oceanographic variables, such as sea surface and air temperatures, wind, pressure, humidity, and cloudiness. The coverage is global and sampling density varies depending on date and geographic position relative to shipping routes and ocean observing systems.

12. Annex B – Ocean Models

Some of the potentially used hydrodynamic models based on EMEC report can be summarized as follows:

Table 3: Common Hydrodynamic models

Models	Dimensions	Grid Structure
ADCIRC	2D/3D	unstructured
ADH	1D/2D/3D	structured
CH2D/CH3D	2D/3D	structured (curvilinear)
DELFT	2D/3D	structured (curvilinear, rectilinear and spherical)
DIVAST	2D	structured
ELCIRC	3D	unstructured, flexible
ELCOM	3D	structured (orthogonal)
GEMSS	1D/2D/3D	
GETM	3D	structured (orthogonal curvilinear)
HRCS	2D/3D	
Mars	2D/3D	structured
Mike Models	1D/2D/3D	structured
RICOM	2D/3D	unstructured
RMA Models	2D/3D	unstructured
ROMS	2D/3D	curvilinear structured
SCHISM	3D	unstructured
SUNTANS	2D/3D	unstructured
TELEMAC	2D/3D	structured
TFD	1D/2D/3D	structured

TRIM	2D/3D	structured
UnTRIM	2D/3D	unstructured

12.1 ADCIRC

Advance Circulation (ADCIRC) is a FORTRAN-based depth-averaged hydrodynamic model (*ADCIRC: An Advanced Three-Dimensional Circulation Model for Shelves, Coasts, and Estuaries. Report 1. Theory and Methodology of ADCIRC-2DDI and ADCIRC-3DL.*, n.d.). It utilizes the finite element method in space allowing the use of highly flexible, unstructured grids. ADCIRC is a highly developed Ocean model for solving the equations of motion for a moving fluid on a rotating earth. These equations were formulated using the traditional hydrostatic pressure and Boussinesq approximations and were discretized in space using the finite element (FE) method and in time using the finite difference (FD) method. ADCIRC can be run either as a two-dimensional depth-integrated (2DDI) model or as a three-dimensional (3D) model. In either case, elevation is obtained from the solution of the vertically integrated continuity equation in Generalized Wave-Continuity Equation (GWCE) form. Velocity is obtained from the solution of either the 2DDI or 3D momentum equations (Luettich & Westerink, 2004). All nonlinear terms have been retained in these equations.

The vertically integrated continuity equation is as follows (Luettich & Westerink, 2004):

$$\frac{\partial H}{\partial t} + \frac{\partial}{\partial x}(UH) + \frac{\partial}{\partial y}(VH) = 0$$

Where,

U, V are depth-averaged velocities in the x, y directions.

H is total water column thickness.

The vertically integrated momentum equations are as follows [24]:

$$\frac{\partial U}{\partial t} + U\frac{\partial U}{\partial x} + V\frac{\partial V}{\partial y} - fV = -g\frac{\partial[\varsigma + \frac{P_s}{g\rho_o} - \alpha\eta]}{\delta x} + \frac{\tau_{xx}}{H\rho_o} - \frac{\tau_{bx}}{H\rho_o} + \frac{M_x}{H} - \frac{D_x}{H} - \frac{B_x}{H}$$

$$\frac{\partial V}{\partial t} + U\frac{\partial V}{\partial x} + V\frac{\partial V}{\partial y} - fU = -g\frac{\partial[\varsigma + \frac{P_s}{g\rho_o} - \alpha\eta]}{\delta y} + \frac{\tau_{xy}}{H\rho_o} - \frac{\tau_{by}}{H\rho_o} + \frac{M_y}{H} - \frac{D_y}{H} - \frac{B_y}{H}$$

Where,

D_x and D_y are Momentum Dispersion

M_x and M_y are vertically integrated lateral stress gradient.

B_x and B_y are vertically integrated baroclinic pressure gradient.

ρ_o is the reference density of water.

ρ is time and spatially varying density

τ_{sx}, τ_{sy} = imposed surface stresses

τ_{bx}, τ_{by} = bottom stress components

P_s = atmospheric pressure at the sea surface

η = Newtonian equilibrium tide potential

ADCIRC boundary conditions include:

- specified elevation (harmonic tidal constituents or time series)
- specified normal flow (harmonic tidal constituents or time series)
- zero normal flow
- slip or no slip conditions for velocity.
- external barriers overflow out of the domain
- internal barrier overflow between sections of the domain
- surface stress (wind and/or wave radiation stress)
- atmospheric pressure
- outward radiation of waves (Sommerfeld condition)

ADCIRC can be forced with:

- elevation boundary conditions
- normal flow boundary conditions
- surface stress boundary conditions
- tidal potential
- earth load/self-attraction tide

12.2 CH3D

CH3D is a Curvilinear-grid Hydrodynamics 3D model developed originally by Dr. Y.

Peter Sheng at the Aeronautical Research Associates of Princeton, Inc. (during 1983-1986) (*ADA318516.Pdf*, n.d.). The CH3D model uses a horizontally boundary-fitted curvilinear grid and a vertically sigma grid, and hence is suitable for application to coastal and nearshore waters with complex shoreline and bathymetry. The non-orthogonal grid enables CH3D to more accurately represent the complex geometry than the orthogonal grid, which is used by most other ocean circulation models. The model contains a robust turbulence closure model (Sheng & Villaret, 1989) which enables accurate simulation of stratified flows in estuaries and lakes. Recent enhancements of the model include modeling of aquatic vegetation, modeling of moving shoreline, addition of a sediment transport model, addition of a water quality model, and addition of a light/seagrass model, and parallel computing which leads to significant increase in computational speed. Recent applications have used horizontal grid on the order of 10-20 meters over a 200km x 50km area.

CH3D-IMS, an integrated modeling system based on the curvilinear grid system of CH3D, includes circulation (CH3D), wave, sediment transport (CH3D-SED3D), water quality (CH3D-WQ3D), light attenuation (CH3D-LA), and seagrass models (CH3D-SAV). Additional processes (e.g., surface water - ground water interaction, atmospheric processes, contaminant transport, data assimilation) are being added.

12.3 DELFT

Delft3D is a finite difference code which solves the Navier-Stokes equations under the Boussinesq and shallow water assumptions, in two (2D) or three (3D) dimensions (*Design and Development of DELFT3D and Application to Coastal Morphodynamics*, n.d.). The model is well calibrated and validated for numerous and vastly diverse coastal settings and widely used by coastal research communities around the world. For a 3Dflow simulation, the system of the momentum equations in −x, −y direction reads:

$$\frac{\partial u}{\partial t}+u\frac{du}{dx}+\upsilon\frac{du}{dy}+\frac{\omega}{H}\frac{du}{d\sigma}-f\upsilon=-\frac{1}{\rho_0}P_x+F_x+\frac{1}{H^2}\frac{\partial}{\partial\sigma}\left(\nu_{V,back}\frac{\partial u}{\partial\sigma}\right)$$

$$\frac{\partial \upsilon}{\partial t}+u\frac{d\upsilon}{dx}+\upsilon\frac{d\upsilon}{dy}+\frac{\omega}{H}\frac{d\upsilon}{d\sigma}-fu=-\frac{1}{\rho_0}P_y+F_y+\frac{1}{H^2}\frac{\partial}{\partial\sigma}\left(\nu_{V,back}\frac{\partial \upsilon}{\partial\sigma}\right)$$

where f is the Coriolis parameter; u and _ are the horizontal velocities in −x and −y direction; ω is the vertical velocity in relation to σ-coordinates; $V_{V,back}$ is the minimum

vertical eddy viscosity; P_x, P_y are the horizontal pressure terms approximated by the Boussinesq assumptions; ρ_0 is the reference water density; $H = d + \zeta$ with d the water depth below a reference level z = 0 and ζ the free surface elevation above that reference level and F_x, F_y are the viscous forces presenting the unbalance of the Reynold's shear stresses. For large-scale problems as in present model set up, the Reynold's stresses along the closed model domain boundaries are neglected (free-slip conditions) and viscous forces terms reduce to the Laplace operator. Under the shallow water assumption, the vertical momentum equation reduces to the hydrostatic pressure assumption where accelerations from buoyancy terms and abrupt variations in com-plex topographic features are assumed to be small in comparison to gravitational acceleration. The resulting expression is:

$$\frac{\partial P}{\partial \sigma} = -\rho g H$$

From the integral form of Eq. and for constant water density ρ,the pressure gradients in −x, −y direction read:

$$\frac{1}{\rho_0} P_x = g\frac{d\zeta}{dx} + \frac{1}{\rho_0}\frac{\mathrm{dP_{atm}}}{\mathrm{dx}}$$

$$\frac{1}{\rho_0} P_y = g\frac{d\zeta}{dy} + \frac{1}{\rho_0}\frac{\mathrm{dP_{atm}}}{\mathrm{dy}}$$

where P_{atm} is the atmospheric pressure term. The free surface elevation ζ is computed from the depth-averaged continuity equation neglecting the contributions due to discharge/removal of water per unit surface area and evaporation/precipitation effects. So:

$$\frac{\partial \zeta}{\partial \mathrm{t}} + \frac{\mathrm{dHU}}{\mathrm{dx}} + \frac{\mathrm{dHV}}{\mathrm{dy}} = 0$$

where U and V are the depth-averaged horizontal velocities in −x and −y direction. An Alternating Direction Implicit (ADI) time integration technique is used to solve the continuity and momentum conservation equations. The accuracy of the ADI solver depends on the Courant-Friedrich-Lewy (CFL) number. In most practical applications as in present study, the CFL number should not exceed a value of 10 but may be higher in case of small variations in space and time. The horizontal advective terms in the momentum equations are discretized in space with the higher-order dissipative

Cyclic scheme which converges well for large time steps, where advection Courant numbers exceed unity .In vertical direction, turbulent flows are resolved by applying the κ-epsilon turbulence closure model (TCM). The horizontal eddy viscosity term which represents the turbulent length scales generated by the flow in the horizontal direction is finally approached by a constant background value ($v_{H,back}$) and the computed, from the TCM, vertical eddy viscosity (v3D) at each σ-layer. The background eddy viscosity value ($v_{H,back}$) may vary with decreasing grid resolution from 1 to 100 m^2s^{-1}.

12.4 ELCIRC

ELCIRC is an unstructured-grid model designed for the effective simulation of 3D baroclinic circulation across river-to-ocean scales (Y. Zhang & Baptista, 2004). It uses a finite-volume/finite-difference Eulerian-Lagrangian algorithm to solve the shallow water equations, written to realistically address a wide range of physical processes and of atmospheric, ocean and river forcings. The numerical algorithm is low order, but volume conservative, stable and computationally efficient. It also naturally incorporates wetting and drying of tidal flats. ELCIRC has been extensively tested against standard ocean/coastal benchmarks and is starting to be applied to estuaries and continental shelves around the world.

12.5 ELCOM

ELCOM (Estuary and Lake Computer Model) is a numerical modeling tool that applies hydrodynamic and thermodynamic models to simulate the temporal behavior of stratified water bodies with environmental forcing (Hodges, 2000). The hydrodynamic simulation method solves the unsteady, viscous Navier-Stokes equations for incompressible flow using the hydrostatic assumption for pressure. Modeled and simulated processes include baroclinic and barotropic responses, rotational effects, tidal forcing, wind stresses, surface thermal forcing, inflows, outflows, and transport of salt, heat and passive scalars. Through coupling with the CAEDYM (Computational Aquatic Ecosystem DYnamics Model) water quality module, ELCOM can be used to simulate three-dimensional transport and interactions of flow physics, biology and chemistry. The hydrodynamic algorithms in ELCOM are based on the Euler-Lagrange method for advection of momentum with a conjugate-gradient solution for the free-surface height. Passive and active scalars (i.e., tracers, salinity and temperature) are

advected using a conservative ULTIMATE QUICKEST discretization.

12.6 MIKE

MIKE 3 Flow Model FM is a modelling system based on a flexible mesh approach. The modelling system has been developed for applications within oceanographic, coastal and estuarine environments (*Identification of Characteristics Influencing Wave Height and Current Velocity in MIKE Model for Simulation of Wind-Induced Ocean Currents and Waves in Southeast of Caspian Sea*, n.d.). The Hydrodynamic Module is based on the numerical solution of the three-dimensional incompressible Reynolds averaged Navier-Stokes equations invoking the assumptions of Boussinesq. Both the full 3D Navier-Stokes equations and the 3D shallow water equations can be applied. The latter invokes the hydrostatic pressure assumption. Thus, the model consists of continuity, momentum, temperature, salinity and density equations and is closed by a turbulent closure scheme. In the horizontal domain both Cartesian and spherical coordinates can be used. The free surface is taken into account using a sigma-coordinate transformation approach. The spatial discretization of the governing equations in conserved form is performed using a cell-centered finite volume method. The spatial domain is discretized by subdivision of the continuum into non-overlapping element/cells. In the horizontal plane an unstructured grid is used while in the vertical domain a structured discretization is used. The elements can be prisms or bricks whose horizontal faces are triangles and quadrilateral elements, respectively. For the time integration a semi-implicit approach is used where the horizontal terms are treated explicitly, and the vertical terms are treated implicitly. The interface convective fluxes are calculated using an approximate Riemann solver. This shock-capturing scheme enables robust and stable simulation of flows involving shocks or discontinuities such as bores and hydraulic jumps.

12.7 RiCOM

The River and Coastal Ocean Model (RiCOM) is a numerical hydrodynamic model used to demonstrate near shore hydrologic conditions primarily surrounding water velocity and height (Walters, 2005).

The interactions of incoming waves/tsunamis with bathymetry, topography and the possible resulting inundation are the primary use of this model. This model has been used in the modelling of many locally sourced tsunami scenarios as well as far field

scenarios. RiCOM was developed by NIWA in an effort to build a framework that could effectively model the behavior, effects, and levels of inundation that coastal New Zealand could expect under different tsunami scenarios. RiCOM operates as a coastal and inundation model within defined boundary conditions for the users chosen study area. RiCOM uses an unstructured, irregular triangular grid to define the study area with varying resolution; often lower resolution in Open Ocean and deeper water with increasing resolution the closer to shore where bathymetry and topography become more of an influence.

The model is based on a standard set of equations - the Reynolds-averaged Navier Stokes equation (RANS) and the incompressibility condition. Due to the model's finite area of processing (output results are for a limited study area), RiCOM is generally used with a Far-field modelling counterpart such as Gerris which will model open ocean behavior (Water Velocities and Height) up to RiCOM grid boundary points where this data will be used as inputs for RiCOM.

12.8 ROMS

ROMS is a three-dimensional, free surface, terrain-following numerical model that solves finite difference approximation of the Reynolds-averaged Navier-Stokes (RANS) equation using the hydrostatic and Boussinesq assumption with split-explicit time stepping algorithm (Shchepetkin & McWilliams, 2005). The governing equations used in ROMS were presented in the form of Cartesian horizontal coordinates and sigma vertical coordinates. For the momentum equations on the x- and y- axis directions are:

$$\frac{\partial(H_z u)}{\partial t}+\frac{\partial(uH_z u)}{\partial x}+\frac{\partial(vH_z u)}{\partial y}+\frac{\partial(\Omega H_z u)}{\partial s}-fH_z v=-\frac{H_z}{\rho_0}\frac{\partial p}{\partial x}-H_z g\frac{\partial \eta}{\partial x}-\frac{\partial}{\partial s}\left(\overline{u'w'}-\frac{v}{H_z}\frac{\partial u}{\partial s}\right)-\frac{\partial(H_z S_{xx})}{\partial x}-\frac{\partial(H_z S_{xy})}{\partial y}+\frac{\partial S_{px}}{\partial s}$$

$$\frac{\partial(H_z v)}{\partial t}+\frac{\partial(uH_z v)}{\partial x}+\frac{\partial(vH_z v)}{\partial y}+\frac{\partial(\Omega H_z v)}{\partial s}-fH_z u=-\frac{H_z}{\rho_0}\frac{\partial p}{\partial y}-H_z g\frac{\partial \eta}{\partial y}-\frac{\partial}{\partial s}\left(\overline{v'w'}-\frac{v}{H_z}\frac{\partial v}{\partial s}\right)-\frac{\partial(H_z S_{yx})}{\partial x}-\frac{\partial(H_z S_{yy})}{\partial y}+\frac{\partial S_{py}}{\partial s}$$

With the hydrostatic equation:

$$0=-\frac{\partial P}{\partial z}-\rho g$$

With the Continuity equation:

$$\frac{\partial \eta}{\partial t} + \frac{\partial (uH_z C)}{\partial x} + \frac{\partial (vH_z u)}{\partial y} + \frac{\partial (H_z \Omega)}{\partial s} = 0$$

and scalar transport:

$$\frac{\partial (H_z C)}{\partial t} + \frac{\partial (uH_z C)}{\partial x} + \frac{\partial (vH_z C)}{\partial y} + \frac{\partial (\Omega H_z C)}{\partial s} = -\frac{\partial}{\partial s}\left(\overline{c'w'} - \frac{v_\theta}{H_z}\frac{\partial C}{\partial s}\right) + C_{source}$$

These equations are closed by parameterizing the Reynolds stresses and turbulent tracer fluxes as

$$\overline{u'w'} = -K_M \frac{\partial u}{\partial z}, \overline{v'w'} = -K_M \frac{\partial v}{\partial z}, \overline{\rho'w'} = -K_M \frac{\partial \rho}{\partial z}$$

Where,

K_M is the eddy viscosity for momentum in m/s

u is the Velocity in x-direction in m/s

v is the velocity in y-direction in m/s

Ω is the velocity in s-direction in m/s

s is the vertical sigma coordinate

z is the vertical elevation in m

η is the wave averaged free surface elevation in m

H_z is the Grid cell thickness in m.

f is the Coriolis parameter s^{-1}

u' is the turbulent velocity in x-direction in m/s.

v' is the turbulent velocity in y-direction in m/s.

w' is the turbulent velocity in s-direction in m/s.

c' is the turbulent concentration in $kg/m^{3.}$

p is the pressure in N/m^2

ρ is the density of seawater in kg/m^3

ρ_o is the reference density of seawater in $kg/m^{3.}$

g is gravity in m/s^2

C is Tracer in kg/m^3

C_{source} is Tracer source/sink term in m/s.

12.9 SCHISM

SCHISM modeling system is a derivative work from the original SELFE model. SELFE was developed at the Oregon Health Sciences University. SCHISM (Semi-implicit

Cross-scale Hydro science Integrated System Model) is an open-source community-supported modeling system based on unstructured grids, designed for seamless simulation of 3D baroclinic circulation across creek-lake-river-estuary-shelf-ocean scales (Y. J. Zhang et al., 2016). It uses a highly efficient and accurate semi-implicit finite-element/finite-volume method with Eulerian-Lagrangian algorithm to solve the Navier-Stokes equations (in hydrostatic form), in order to addresses a wide range of physical and biological processes. The numerical algorithm judiciously mixes higher-order with lower-order methods, to obtain stable and accurate results in an efficient way. Mass conservation is enforced with the finite-volume transport algorithm. It also naturally incorporates wetting and drying of tidal flats.

The SCHISM system has been extensively tested against standard ocean/coastal benchmarks and applied to a number of regional seas/bays/estuaries around the world in the context of general circulation, tsunami and storm-surge inundation, water quality, oil spill, sediment transport, coastal ecology, and wave-current interaction.

Major Characteristics of SCHISM are as follows:

- Finite element/volume formulation
- Unstructured mixed triangular/quadrangular grid in the horizontal dimension
- Hybrid SZ coordinates or new LSC2 in the vertical dimension
- Polymorphism: a single grid can mimic 1D/2DV/2DH/3D configurations
- Semi-implicit time stepping (no mode splitting): no CFL stability constraints → numerical efficiency.
- Robust matrix solver
- Higher-order Eulerian-Lagrangian treatment of momentum advection (with ELAD filter)
- Natural treatment of wetting and drying suitable for inundation studies
- Mass conservative, monotone, higher-order transport solver: TVD2; WENO
- No bathymetry smoothing necessary.
- Very tolerant of bad quality meshes in the non-eddying regime.

12.10 TELEMAC

The TELEMAC-3D code solves such three-dimensional equations as the free surface flow equations (with or without the hydrostatic pressure hypothesis) and the transport-diffusion equations of intrinsic quantities (temperature, salinity, concentration) (Yousef

et al., n.d.). Its main results, at each point in the resolution mesh in 3D, are the velocity in all three directions and the concentrations of transported quantities. Water depth is the major result as regards the 2D surface mesh. The TELEMAC-3D's prominent applications can be found in free surface flow, in both seas and rivers; the software can take the following processes into account:

- Influence of temperature and/or salinity on density,
- Bottom friction,
- Influence of the Coriolis force,
- Influence of weather elements: air pressure, rain or evaporation and wind,
- Consideration of the thermal exchanges with the atmosphere,
- Sources and sinks for fluid moment within the flow domain,
- Simple or complex turbulence models (k-ε) taking the effects of the Archimedean force (buoyancy) into account,
- Dry areas in the computational domain: tidal flats,
- Current drift and diffusion of a tracer, with generation or disappearance terms,
- Oil spill modelling.

The code is applicable to many fields. The main ones are related to the marine environment through the investigations of currents being induced either by tides or density gradients, with or without the influence of such an external force as the wind or the air pressure. It can be applied either to large extent areas (on a sea scale) or to smaller domains (coasts and estuaries) for the impact of sewer effluents, the study of thermal plumes or even sedimentary transport. As regards the continental waters, the study of thermal plumes in rivers, the hydrodynamic behavior or natural or man-made lakes can be mentioned as well. TELEMAC-3D is developed by the LNHE (Laboratoire National d'Hydraulique et Environment) of the Research and Development Division of EDF (EDF-R&D).

12.11 **FVCOM**

FVCOM is a prognostic, unstructured-grid, finite-volume, free-surface, 3-D primitive equation coastal ocean circulation model developed by UMASSD-WHOI joint efforts (*FVCOM (the Unstructured Grid Finite Volume Community Ocean Model) | Model Item | OpenGMS*, n.d.). The model consists of momentum, continuity, temperature, salinity and density equations and is closed physically and mathematically using turbulence

closure submodels. The horizontal grid is comprised of unstructured triangular cells and the irregular bottom is preseented using generalized terrain-following coordinates. The General Ocean Turbulent Model (GOTM) developed by Burchard's research group in Germany has been added to FVCOM to provide optional vertical turbulent closure schemes. FVCOM is solved numerically by a second-order accurate discrete flux calculation in the integral form of the governing equations over an unstructured triangular grid. This approach combines the best features of finite-element methods (grid flexibility) and finite-difference methods (numerical efficiency and code simplicity) and provides a much better numerical representation of both local and global momentum, mass, salt, heat, and tracer conservation. The ability of FVCOM to accurately solve scalar conservation equations in addition to the topological flexibility provided by unstructured meshes and the simplicity of the coding structure has make FVCOM ideally suited for many coastal and interdisciplinary scientific applications. FVCOM was originally developed for the estuarine flooding/drying process in estuaries and the tidal-, buoyancy- and wind-driven circulation in the coastal region featured with complex irregular geometry and steep bottom topography. This model has been upgraded to the spherical coordinate system for basin and global applications.